Journal Name

RSCPublishing

ARTICLE

Electronic Supporting Information for:

Vanadyl phenolate complexes for ring opening homo- and co-polymerisation of ε-caprolactone, *L*-lactide and *rac*-lactide

Feijie Ge,[a] *Yi Dan,*[a] *Yahya Al-Khafaji,*[a] *Timothy J. Prior,*[b] *Long Jiang**[a] , *Mark R.J. Elsegood*[c] *and Carl Redshaw**[b, c]

+

[a] State Key Laboratory of Polymer Materials Engineering of China (Sichuan University), Polymer Research Institute of Sichuan University, Chengdu 610065, Sichuan, China.

[b] Department of Chemistry, University of Hull, Hull, HU6 7RX, UK.

[c] AstaTech Ltd, Chengdu, 611137, Sichuan, China.

Corresponding authors email address: jianglong@scu.edu.cn and C.Redshaw@hull.ac.uk

Contents

Figure S5. ORTEP diagram of the asymmetric unit of complex **6.3CH$_2$Cl$_2$** with ellipsoids at 50 % probability level.

Figure S6. ORTEP diagram of the asymmetric unit of complex **7** with ellipsoids at 50 % probability level.

Table S2. Crystallographic data for complexes **1**, **2**, **3**·2CH$_2$Cl$_2$, **4**·2CH$_2$Cl$_2$, **4**·3CH$_2$Cl$_2$ and **5**·2MeCN.

Figure S7. ^{1}H NMR spectrum of the resulting PCL (run 3, table 3).

Figure S8. ^{1}H NMR spectrum of the resulting PCL (run 27, table 3).

Figure S9. MALDI-ToF spectrum of PCL (run 3, table 3).

Figure S10. MALDI-ToF spectrum of PCL (run 9, table 3).

Figure S11. MALDI-ToF spectrum of PCL (run 22, table 3).

Figure S12. MALDI-ToF spectrum of PCL (run 27, table 3).

Figure S13. MALDI-ToF spectrum of PCL (no solvent run 1, table 4).

Figure S14. MALDI-ToF spectrum of PCL (no solvent run 7, table 4).

Figure S15. Plot of ^{51}V NMR signal (from Table 2) *versus* catalytic activity.

Figure S16. MALDI-ToF spectrum of PLA (run 1, table 5).

Figure S17. MALDI-ToF spectrum of PLA (run 10, table 5).

Figure S18. MALDI-ToF spectrum of PLA (run 24, table 5).

Figure S19. MALDI-ToF spectrum of PLA (run x, table 6).

Figure S20. 2D J-resolved ^{1}H NMR spectrum of PLA (run 1, table 6).

Figure S21. 2D J-resolved ^{1}H NMR spectrum of PLA (run 5, table 6).

Figure S22. 2D J-resolved ^{1}H NMR spectrum of PLA (run 17, table 6).

Figure S23. ^{1}H NMR spectrum of co-polymer from CL and *L*-LA (run 4, table 7).

Figure S24. DSC plot of co-polymer from CL and *L*-LA (run 4, table 7).

Figure S25. ^{1}H NMR spectrum of co-polymer from CL and *rac*-LA (run 6, table 8).

Figure S26. DSC plot of co-polymer from CL and *rac*-LA (run 4, table 8).

Figure S 27. GPC run 1 table 7.

Figure S 28. GPC run 2 table 7.

Figure S 29. GPC run 3 table 7.

Figure S 30. GPC run 4 table 7.

Figure S 31. GPC run 5 table 7.

Figure S 32. GPC run 6 table 7.

Figure S 33. GPC run 7 table 7.

Figure S 34. GPC run 1 table 8.

Figure S 35. GPC run 2 table 8.

Figure S 36. GPC run 3 table 8.

Figure S 37. GPC run 4 table 8.

Figure S 38. GPC run 5 table 8.

Figure S 39. GPC run 6 table 8.

Figure S 40. GPC run 7table 8.

D—H···*A*	*D*—H	H···*A*	*D*···*A*	*D*—H···*A*
C73—H73*A*···O7	0.99	2.23	3.09 (2)	144

Table S1. H-bonding geometry in **6**.

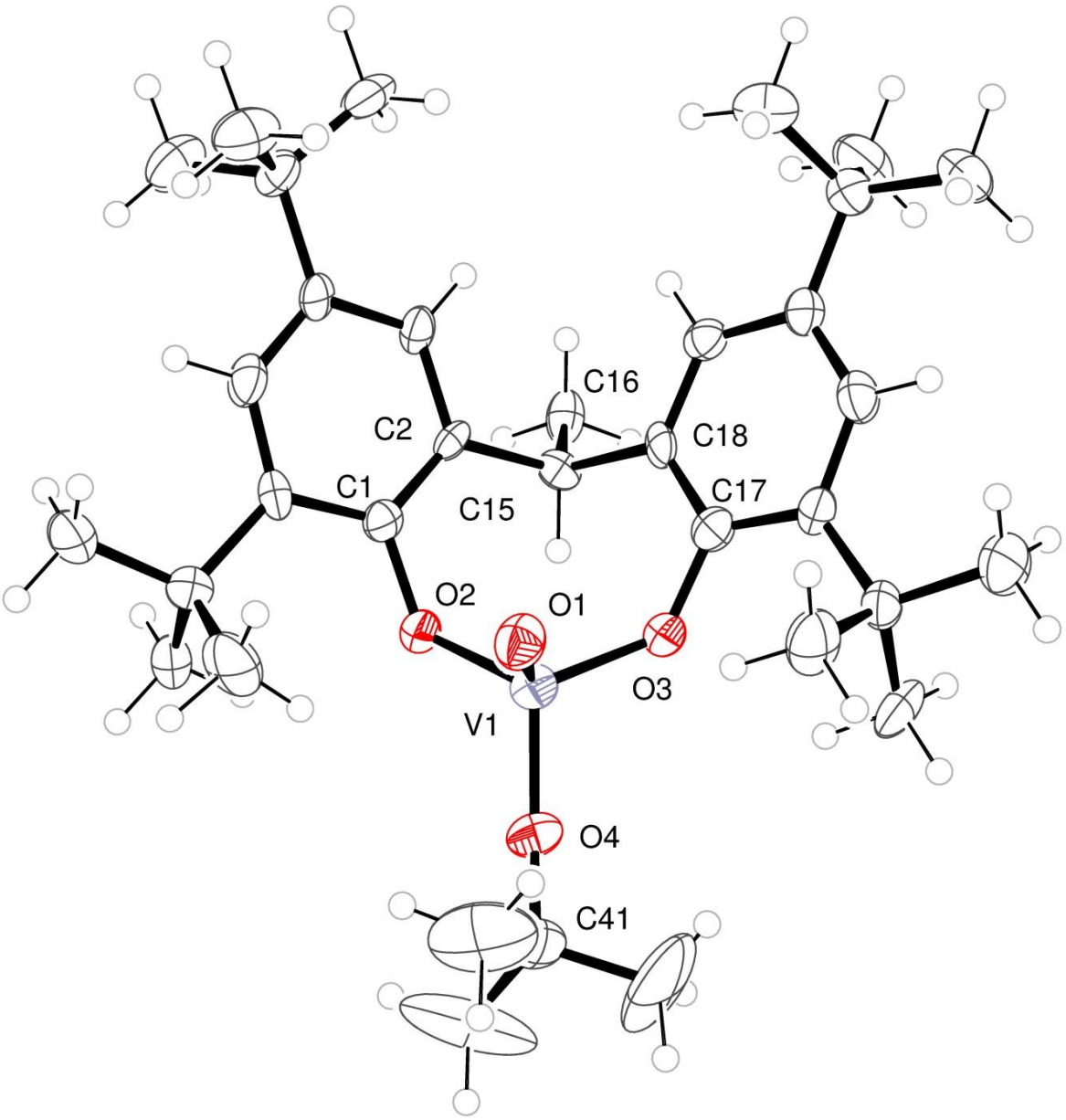

Figure S1. ORTEP diagram of the asymmetric unit of complex **1** with ellipsoids drawn at 50 % probability level.

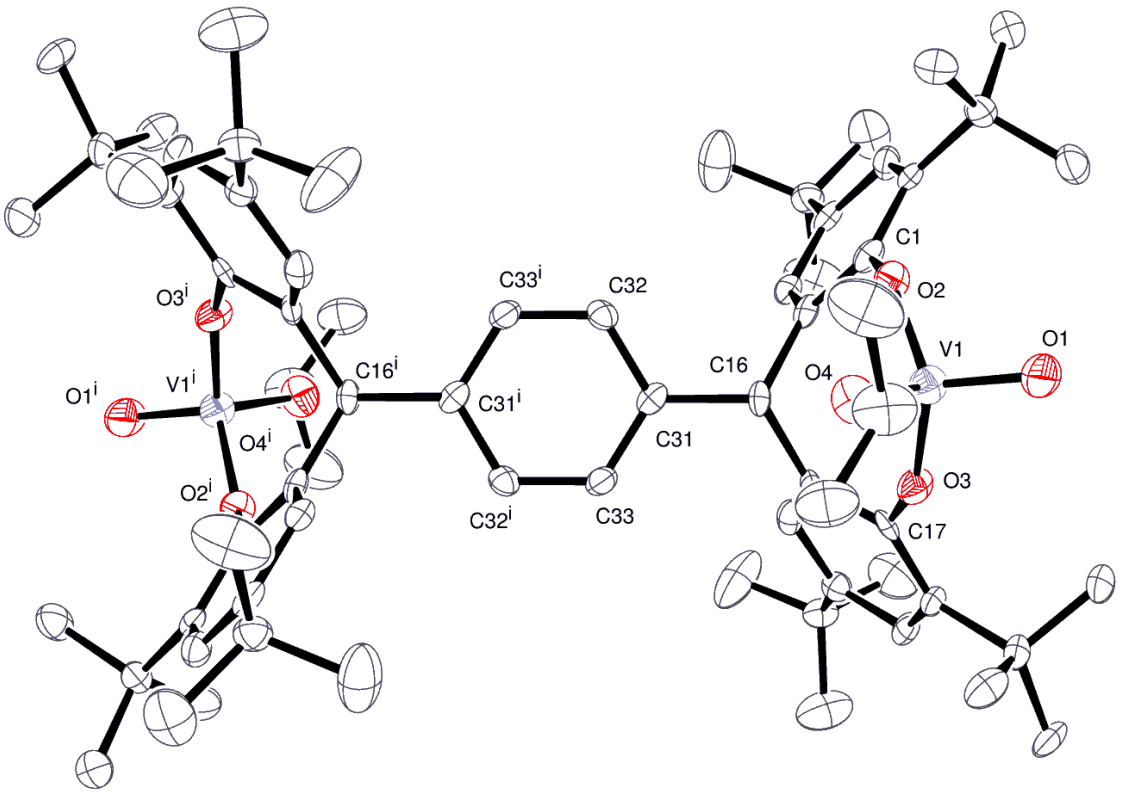

Figure S2. ORTEP diagram of complex **4** with ellipsoids drawn at 50 % probability level. Symmetry equivalent atoms are generated by the operator $i = -x, 1-y, 1-z$. In the interest of clarity, hydrogen atoms are omitted.

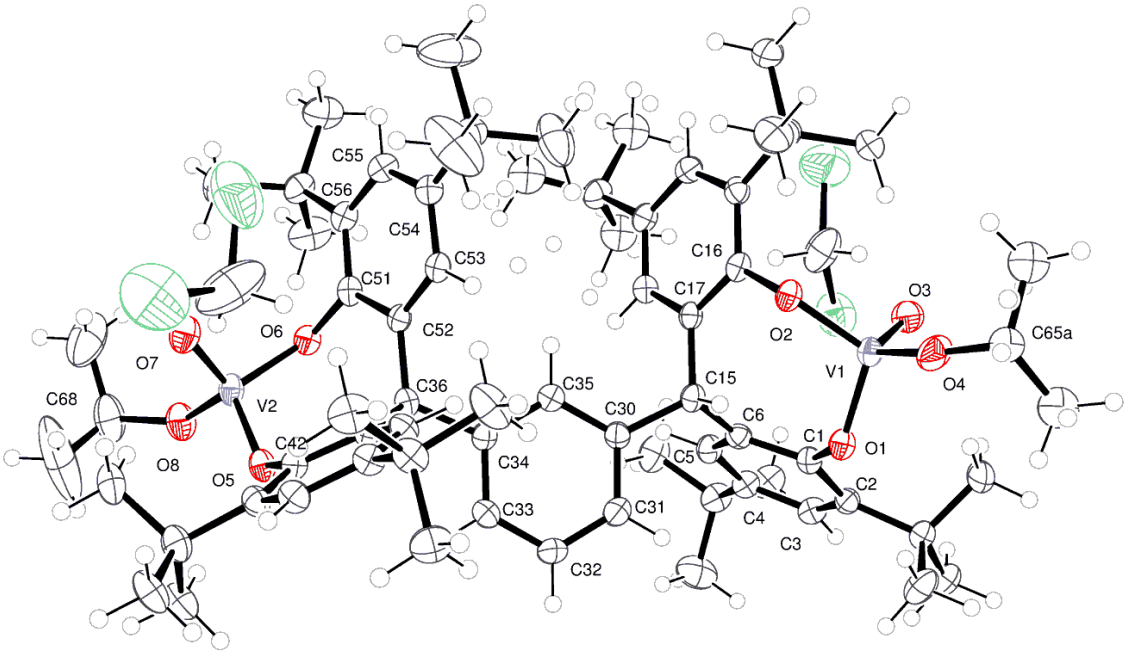

Figure S3. ORTEP diagram of the asymmetric unit of complex **5** with ellipsoids at 50 % probability level.

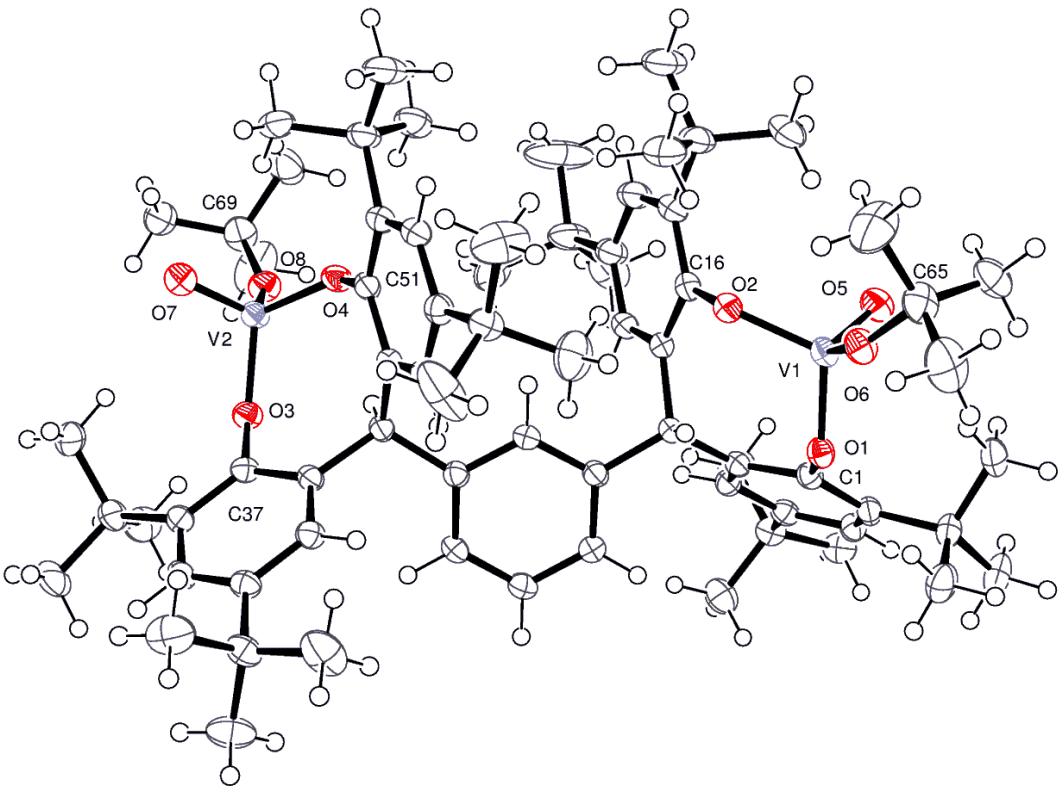

Figure S4. **.** ORTEP diagram of the asymmetric unit of complex **6.2CH$_2$Cl$_2$** with ellipsoids at 50 % probability level.

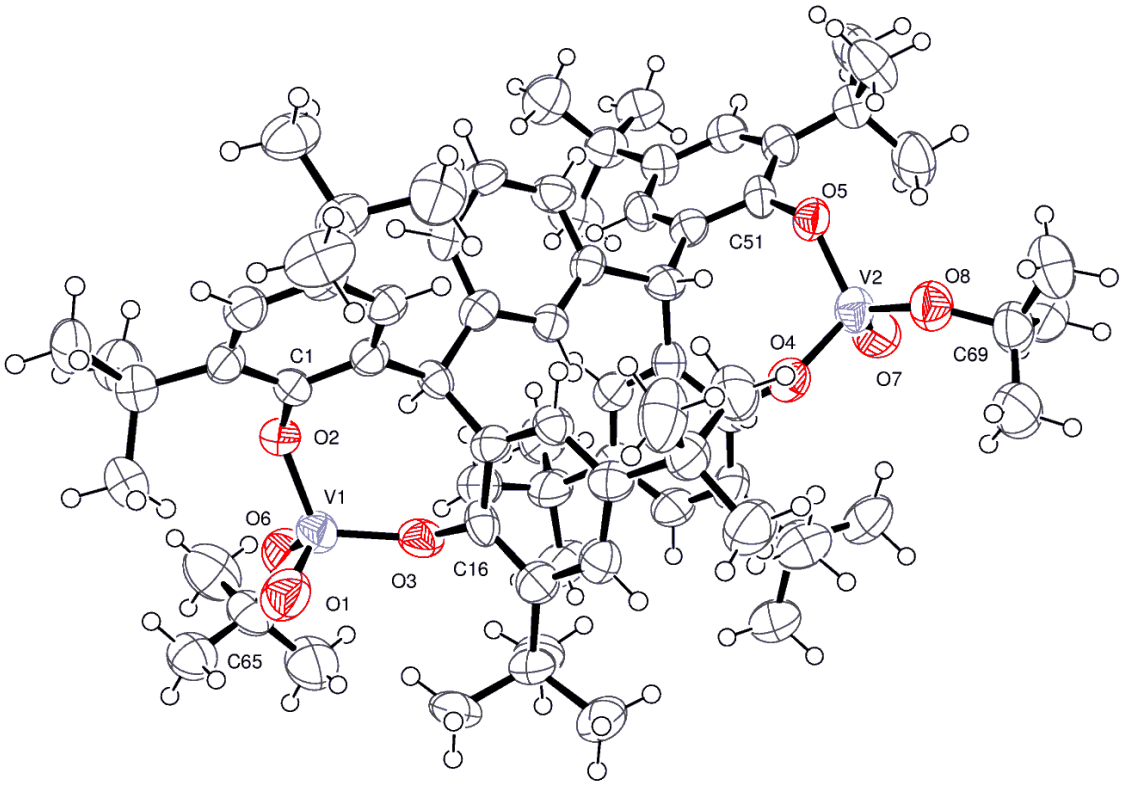

Figure S5. ORTEP diagram of the asymmetric unit of complex **6.3CH$_2$Cl$_2$** with ellipsoids at 50 % probability level.

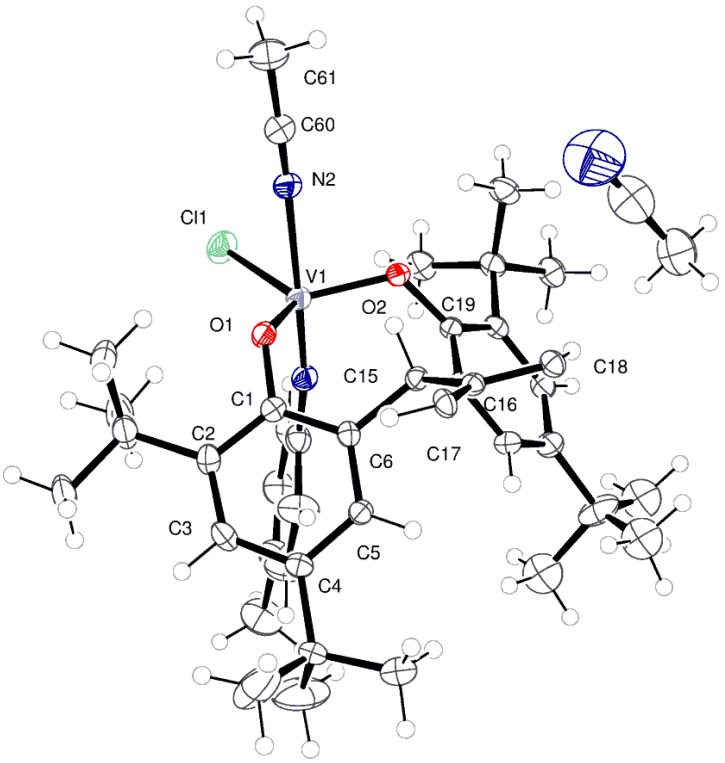

Figure S6. ORTEP diagram of the asymmetric unit of complex **7** with ellipsoids at 50 % probability level.

Compound	**1**	**2**	**3**·2CH_2Cl_2
Formula	$C_{34}H_{53}O_2V$	$C_{70}H_{100}O_8V_2$	$C_{70}H_{100}O_8V_2.2(CH_2Cl_2)$
Formula weight	576.70	1171.37	1339.21
Crystal system	Monoclinic	Monoclinic	Orthorhombic
Space group	*P*2$_1$/*c*	*P*2$_1$/*c*	*P*bca
a (Å)	13.886(8)	10.967(4)	11.0268(7)
b (Å)	23.550(14)	10.344(3)	19.1028(13)
c (Å)	10.938(7)	27.9706(10)	70.103(5)
α (º)			90
β (º)	110.492(8)	92.329(6)	90
γ (º)			90
V (Å^3)	3351(4)	3170.4(15)	14766.7(17)
Z	4	2	8
Temperature (K)	150(2)	100(2)	100(2)
Wavelength (Å)	0.71075	0.71075	0.71075
Calculated density (g.cm^{-3})	1.143	1.227	1.205
Absorption coefficient (mm^{-1})	0.329	0.349	0.448
Transmission factors (min./max.)	0.502 and 1.000	0.600 and 1.000	0.682 and 1.000
Crystal size (mm)	0.06× 0.01 × 0.01	0.09 × 0.03 × 0.01	0.27 × 0.10 × 0.02
θ(max) (°)	25.171	25.095	27.507
Reflections measured	37155	17727	91884
Unique reflections	5977	5568	16405
R_{int}	0.3338	0.1786	0.0794
Reflections with $F^2 > 2\sigma(F^2)$	2250	2591	11323
Number of parameters	368	372	763
R_1 [$F^2 > 2\sigma(F^2)$]	0.0922	0.0987	0.0723
wR_2 (all data)	0.2193	0.2427	0.2255
GOOF, *S*	1.016	1.058	1.043
Largest difference peak and hole (e Å^{-3})	0.323 and –0.321	0.585 and –0.489	0.624 and -1.154

Compound	**4**·2CH_2Cl_2	**4**·3CH_2Cl_2	**5**·2MeCN
Formula	$C_{72}H_{104}O_8V_2.2(CH_2Cl_2)$	$C_{71}H_{102}O_8V_2\cdot 3(CH_2Cl_2)$	$C_{82}H_{106}Cl_2N_4O_4V_2\cdot 2(MeCN)$
Formula weight	1369.28	1440.18	1466.59
Crystal system	Monoclinic	Monoclinic	Monoclinic
Space group	$P2_1/n$	$P2_1/n$	$P2_1/n$
a (Å)	21.4616(15)	21.479(15)	10.6773(7)
b (Å)	14.3723(10)	14.382(9)	18.5913(13)
c (Å)	25.6780(18)	25.952(18)	21.2520(15)
α (°)			90
β (°)	104.267(1)	103.682(7)	96.0750(10)
γ (°)			90
V (Å^3)	7676.2(9)	7789(9)	4194.9(5)
Z	4	4	2
Temperature (K)	100	100	100(2)
Wavelength (Å)	0.71073	0.6889	0.71073
Calculated density (g.cm^{-3})	1.185	1.228	1.161
Absorption coefficient (mm^{-1})	0.43	0.46	0.337
Transmission factors (min./max.)	0.678 and 1.000	0.947 and 0.982	0.754 and 1.000
Crystal size (mm)	0.10 × 0.07 × 0.02	0.12 × 0.05 × 0.04	0.20 × 0.03 × 0.03
θ(max) (°)	27.5	22.5	27.609
Reflections measured	91396	50369	14230
Unique reflections	17489	11066	14230
R_{int}	0.073	0.196	0.0798
Reflections with $F^2 > 2\sigma(F^2)$	13364	6500	12276
Number of parameters	794	889	453
R_1 [$F^2 > 2\sigma(F^2)$]	0.054	0.128	0.0736
wR_2 (all data)	0.162	0.370	0.1911
GOOF, S	1.04	1.03	1.109
Largest difference peak and hole (e Å^{-3})	0.86 and –0.41	0.78 and –0.67	0.808 and -0.535

Table S2. Crystallographic data for complexes **1**, **2**, **3**·2CH_2Cl_2, **4**·2CH_2Cl_2, **4**·3CH_2Cl_2 and **5**·2MeCN.

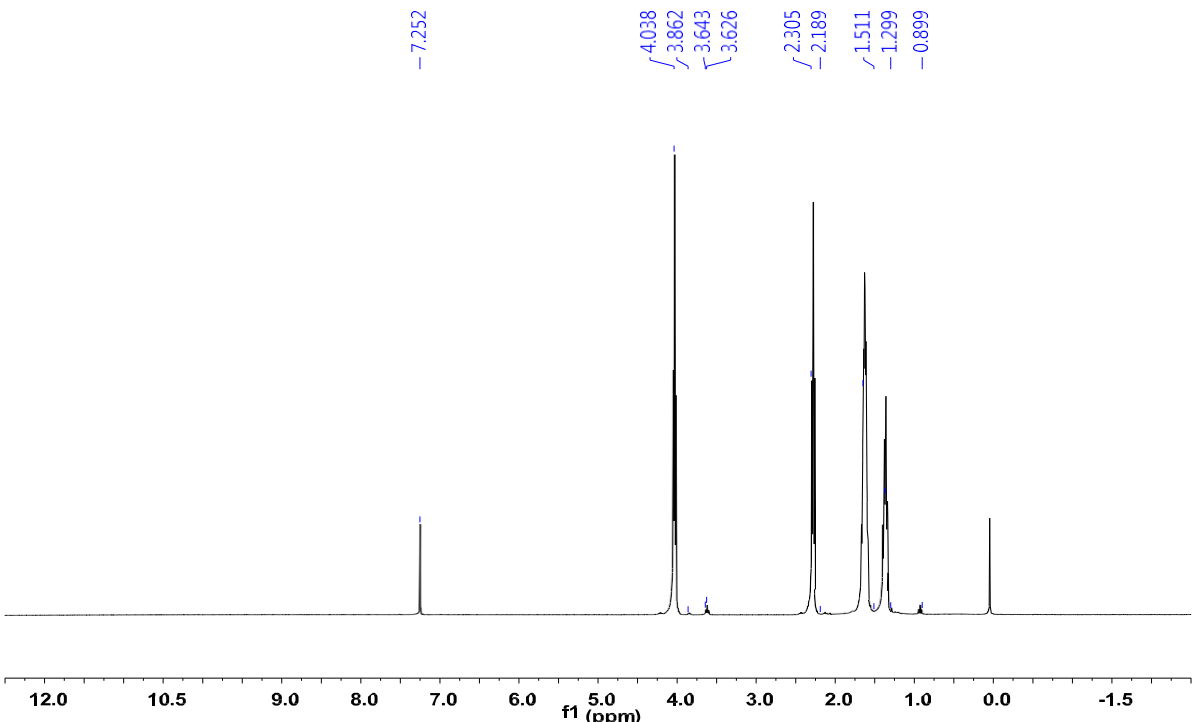

Figure S7. ^{1}H NMR spectrum of the resulting PCL (run 3, table 3).

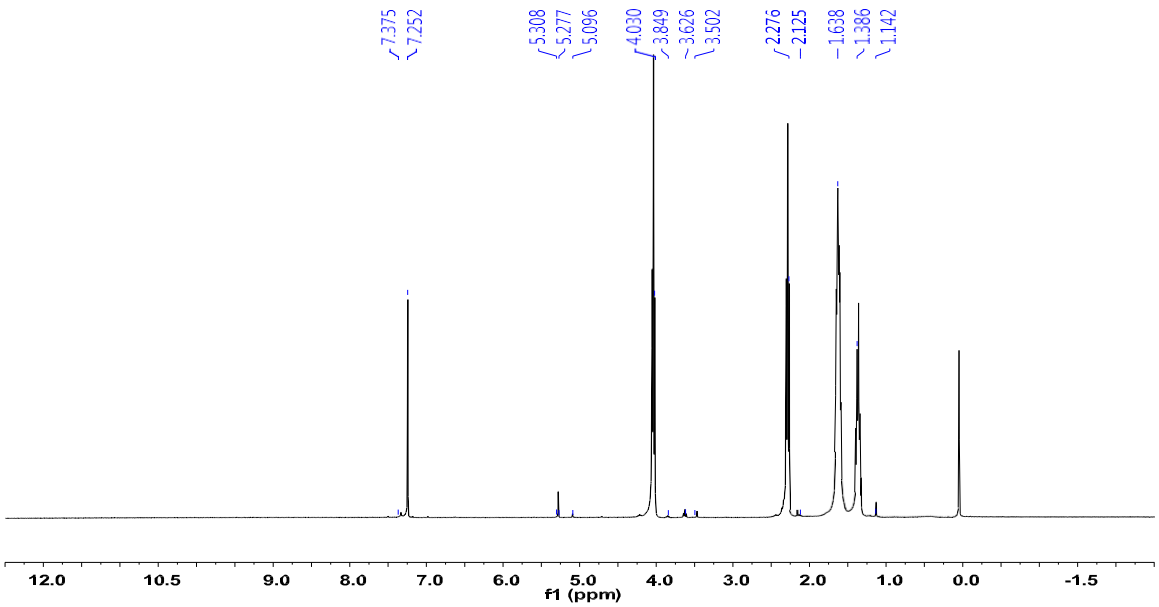

Figure S8. ^{1}H NMR spectrum of the resulting PCL (run 27, table 3).

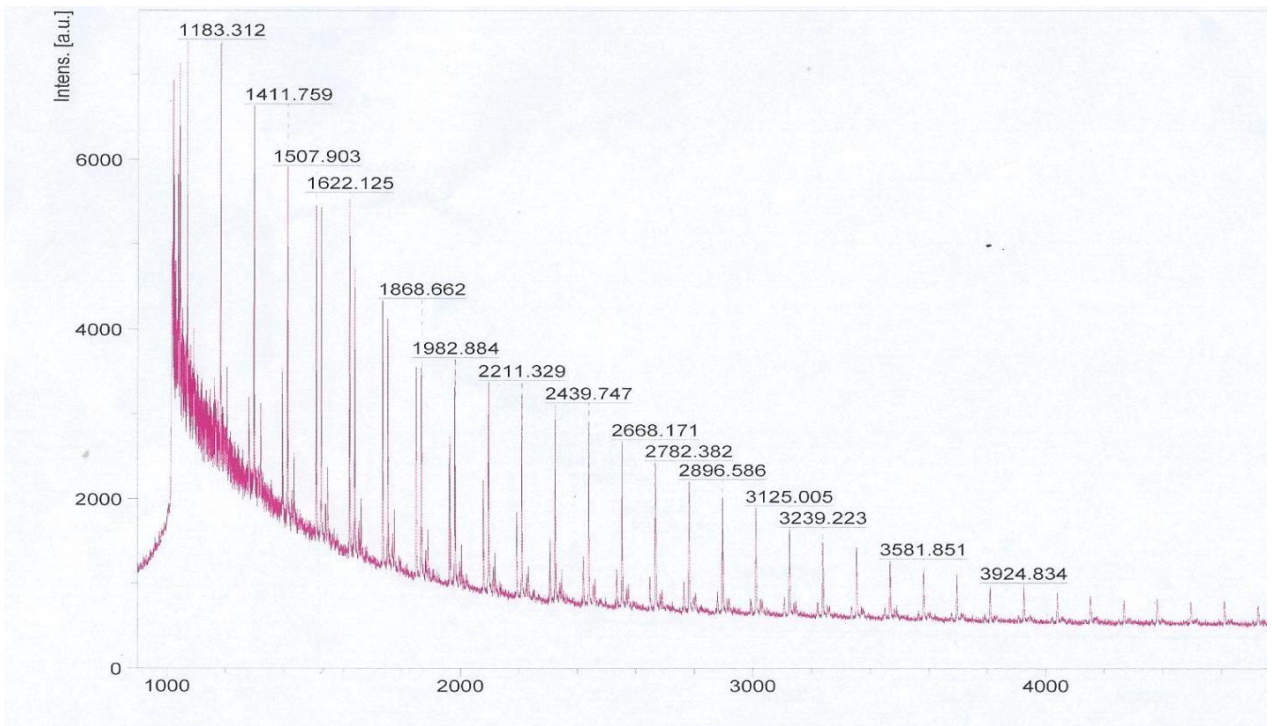

Figure S9. MALDI-ToF spectrum of PCL (run 3, table 3).

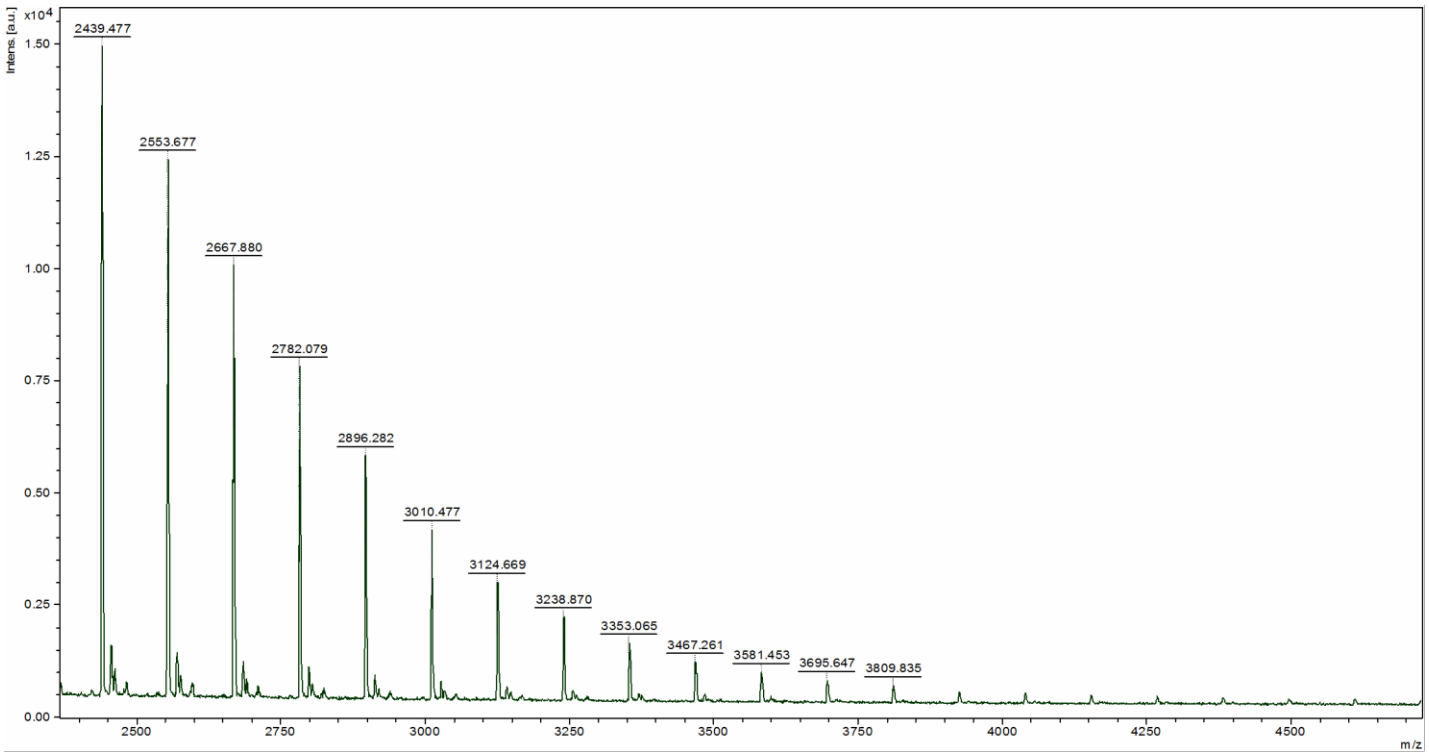

Figure S10. MALDI-ToF spectrum of PCL (run 9, table 3).

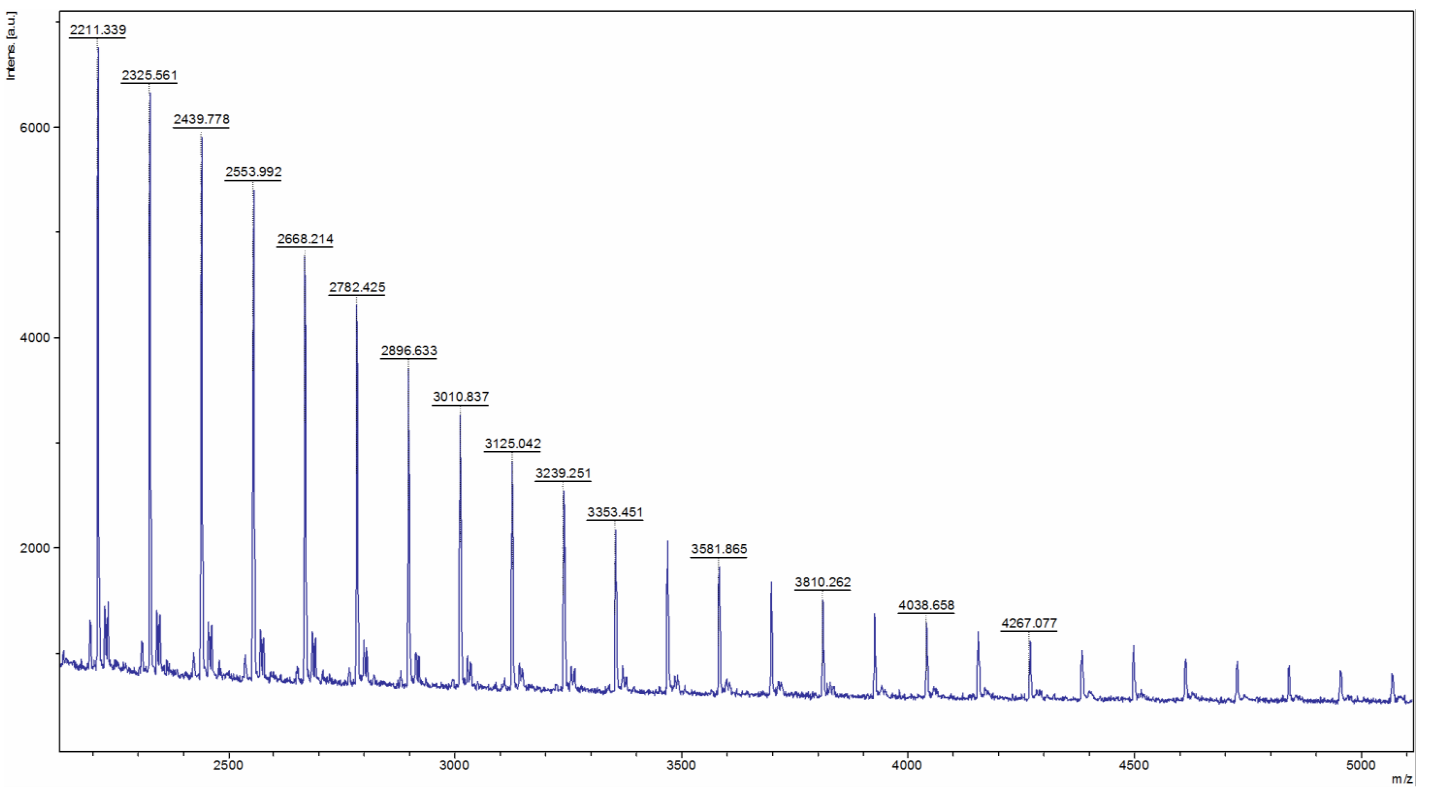

Figure S11. MALDI-ToF spectrum of PCL (run 22, table 3).

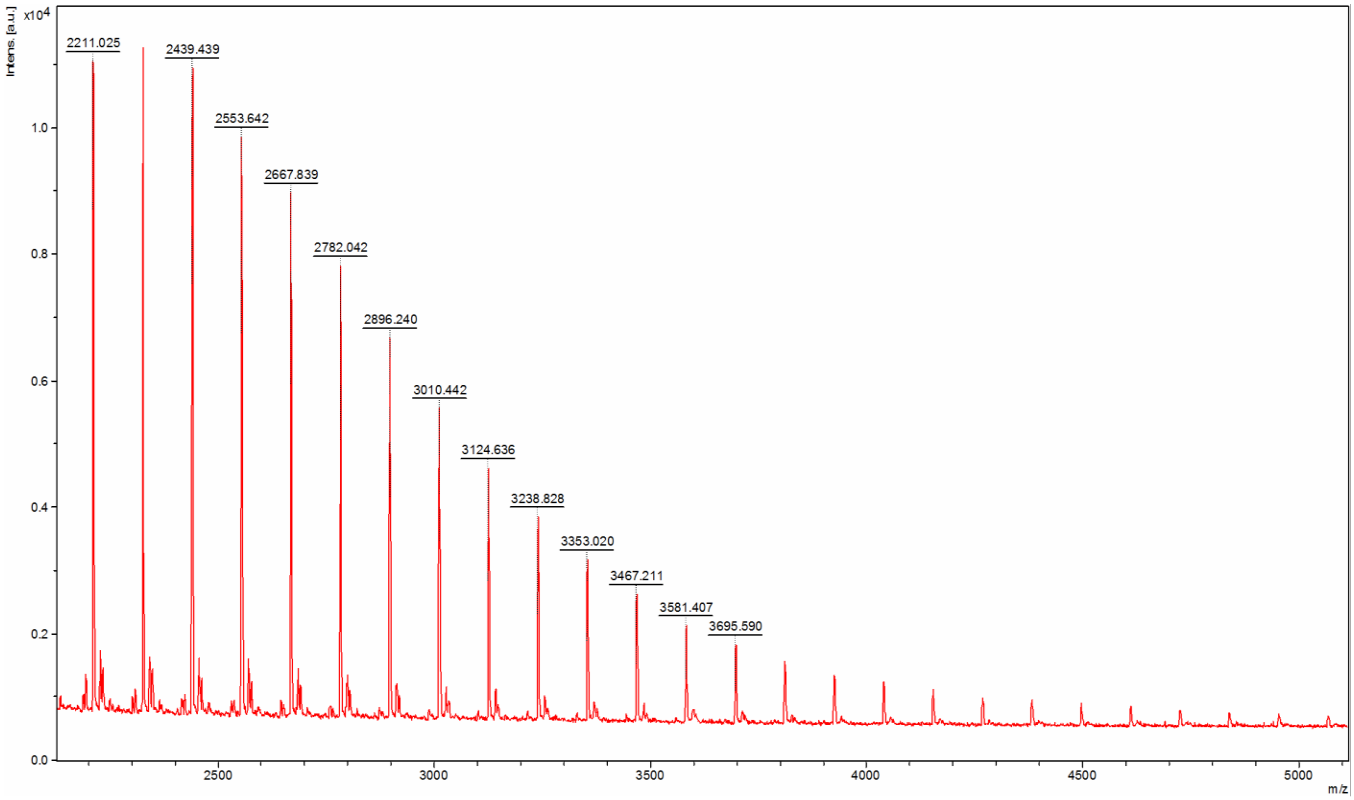

Figure S12. MALDI-ToF spectrum of PCL (run 27, table 3).

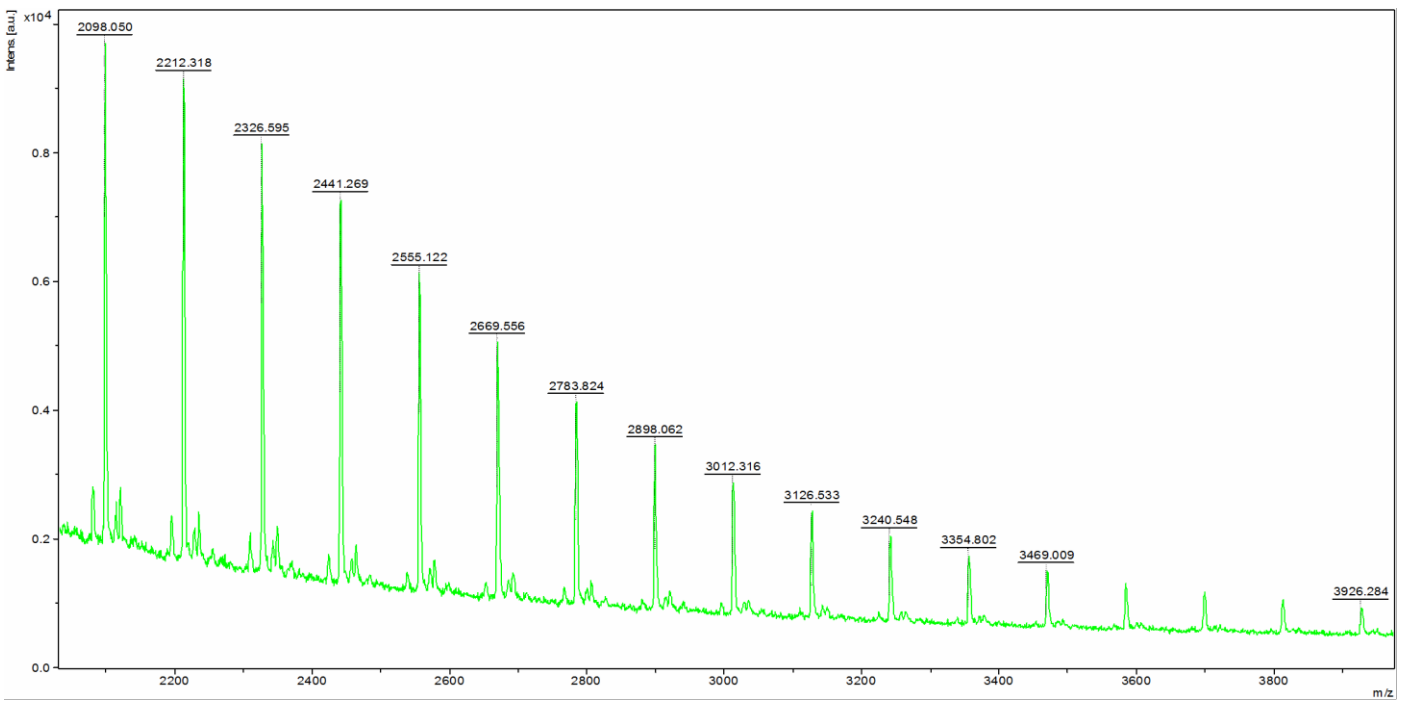

Figure S13. MALDI-ToF spectrum of PCL (no solvent run 1, table 4).

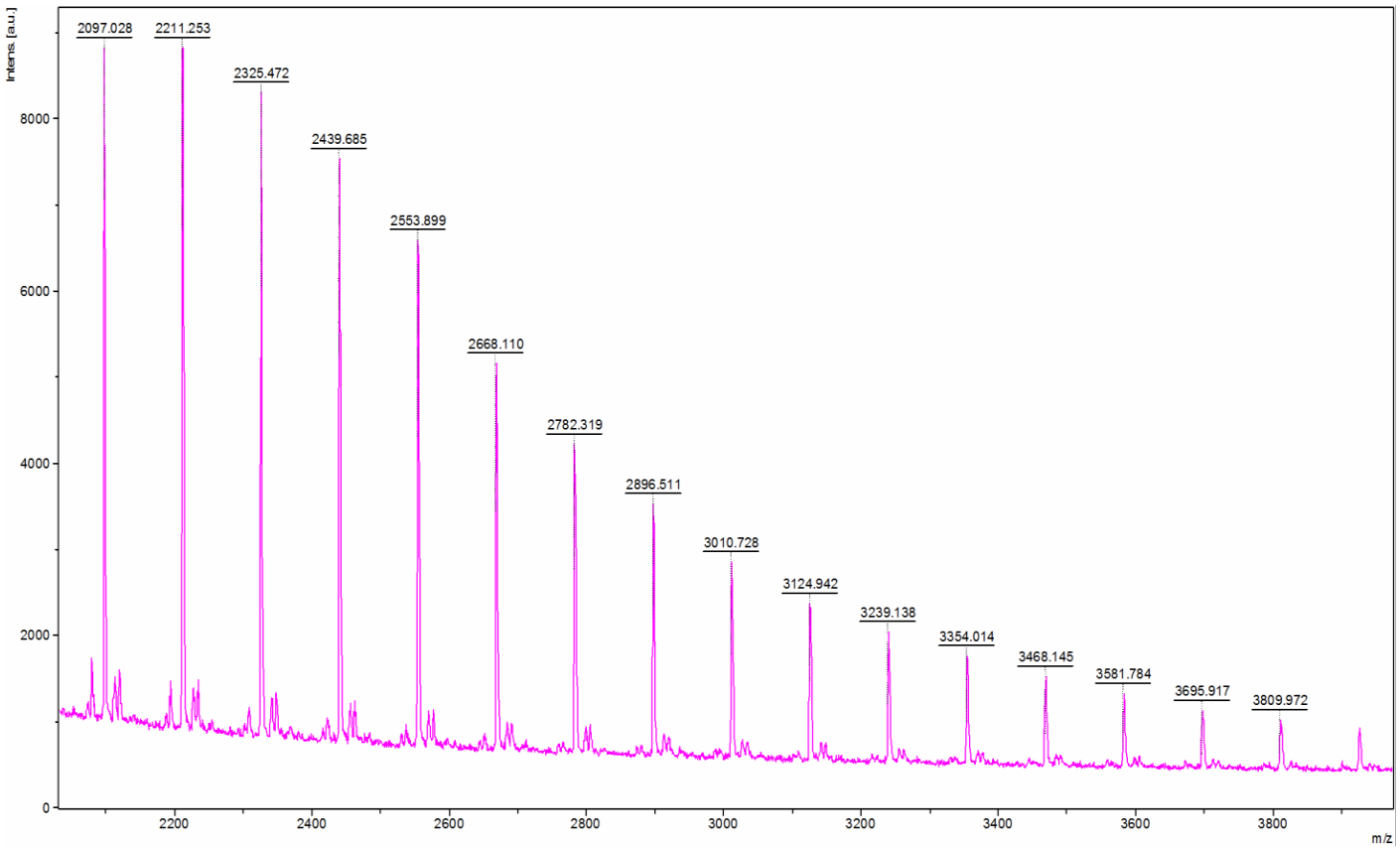

Figure S14. MALDI-ToF spectrum of PCL (no solvent run 7, table 4).

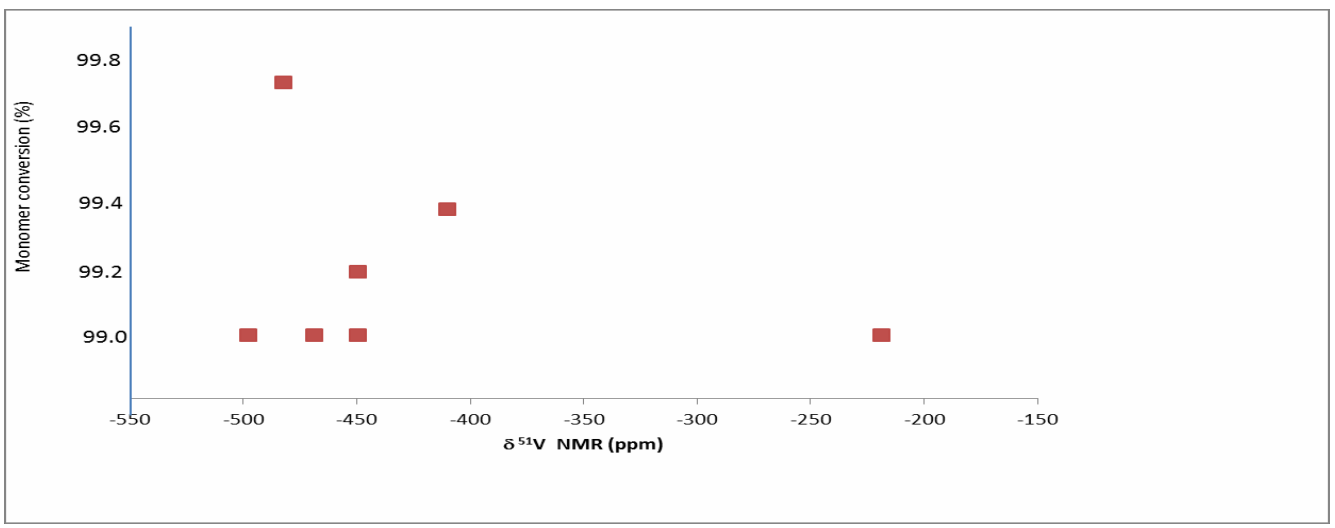

Figure S15. Plot of ^{51}V NMR signal (from Table 2) *versus* catalytic activity.

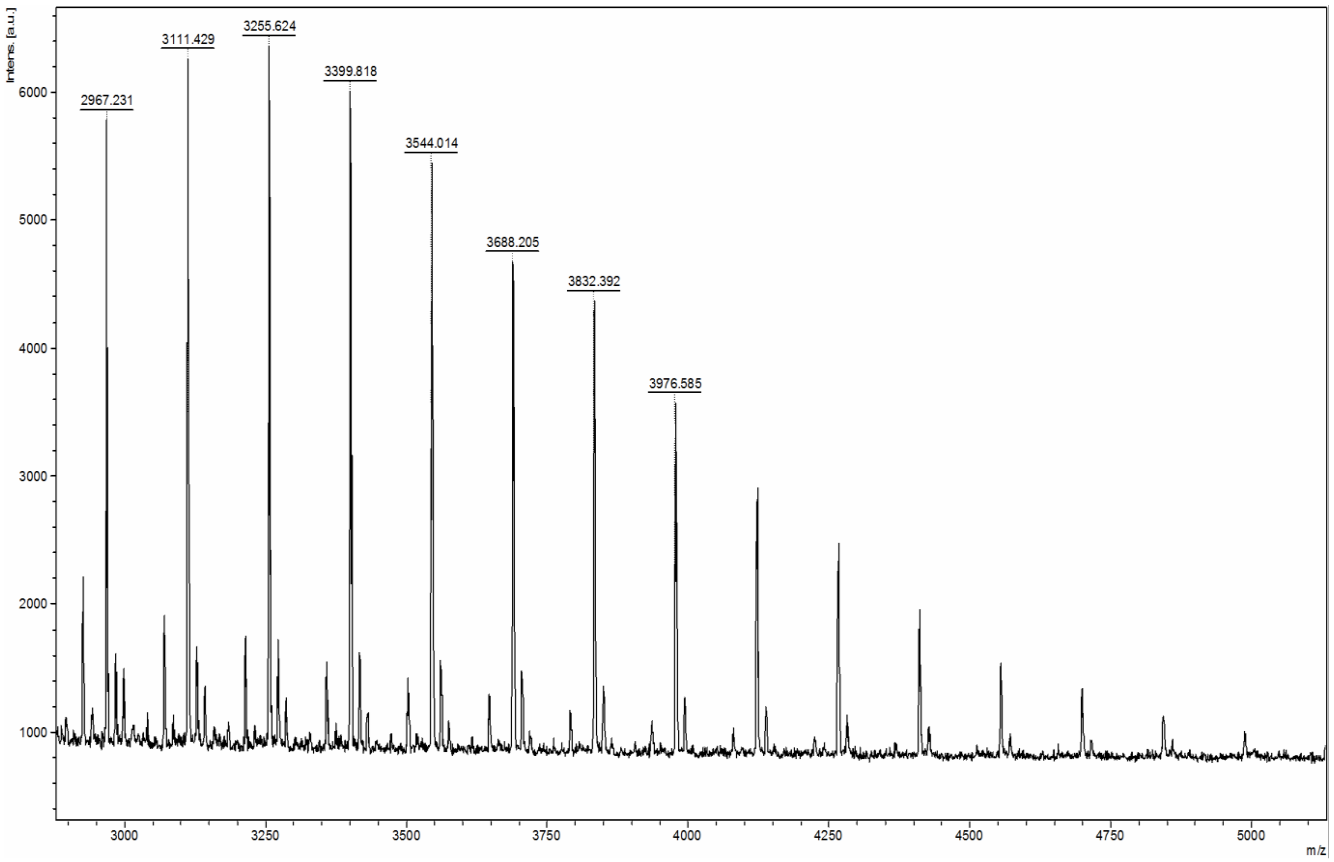

Figure S16. MALDI-ToF spectrum of PLA (run 1, table 5).

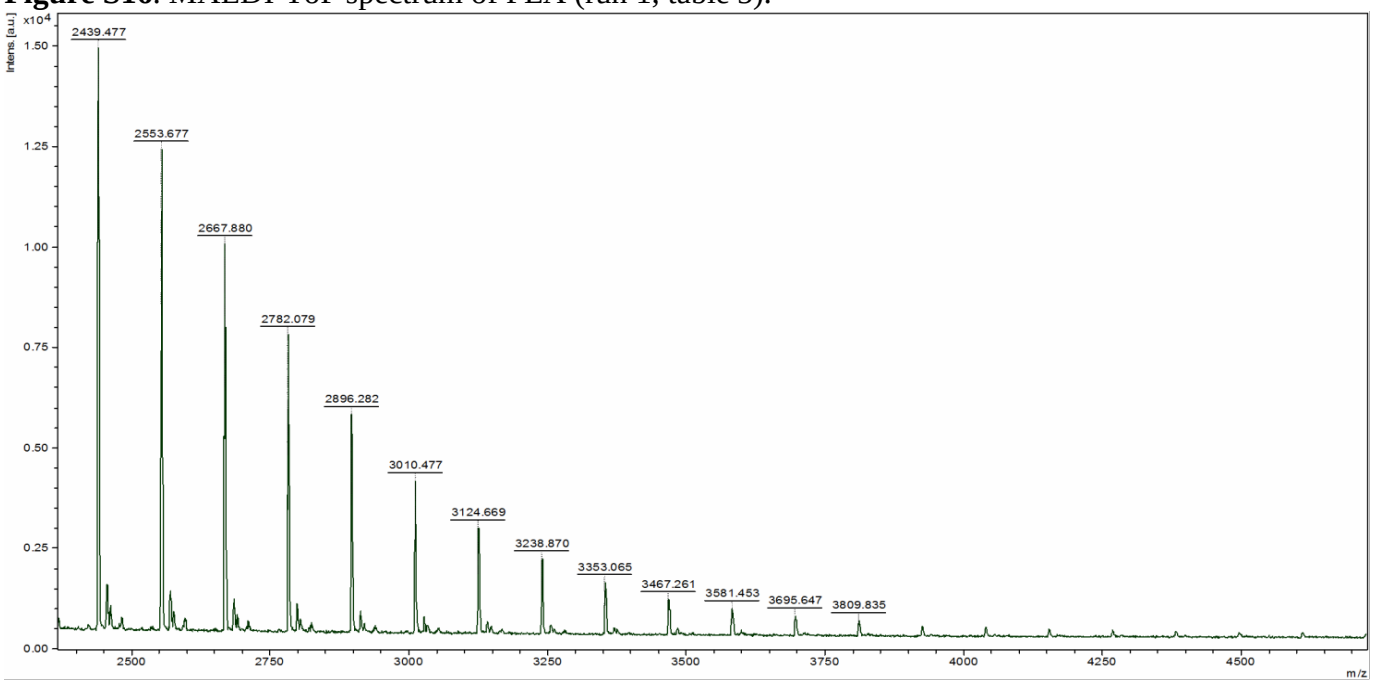

Figure S17. MALDI-ToF spectrum of PLA (run 10, table 5).

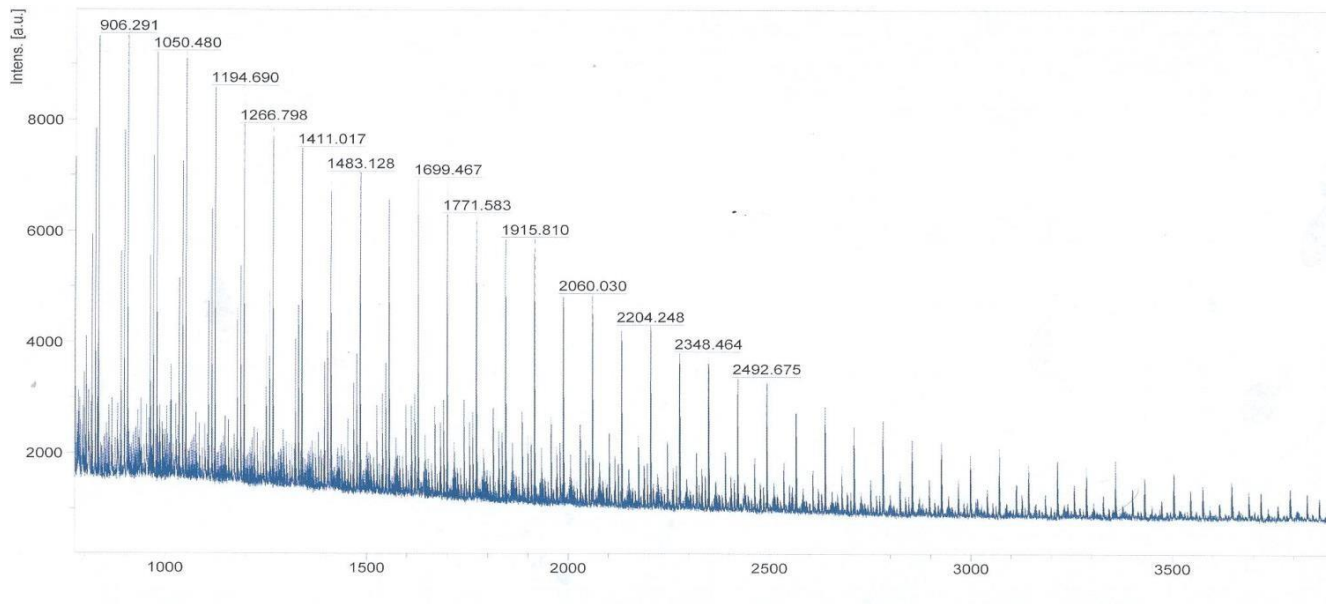

Figure S18. MALDI-ToF spectrum of PLA (run 24, table 5).

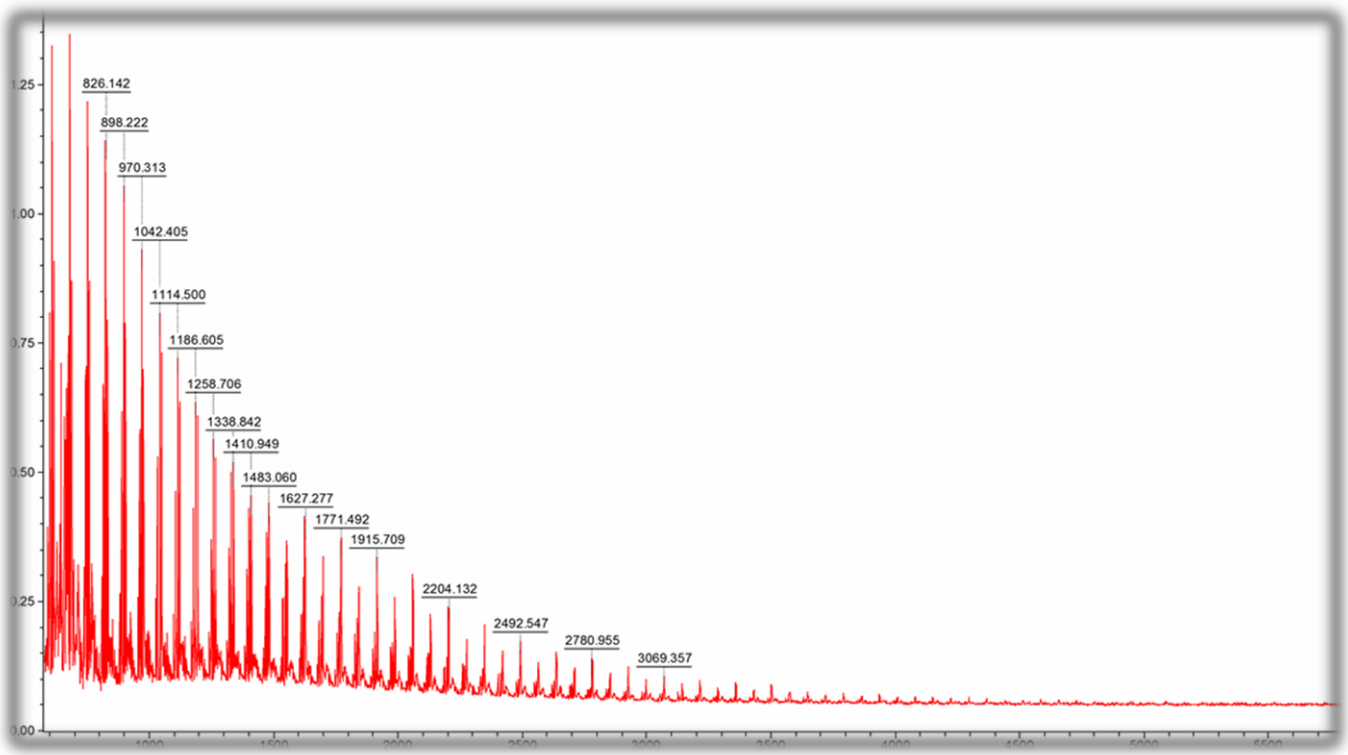

Figure S19. MALDI-ToF spectrum of PLA (run 19, table 6).

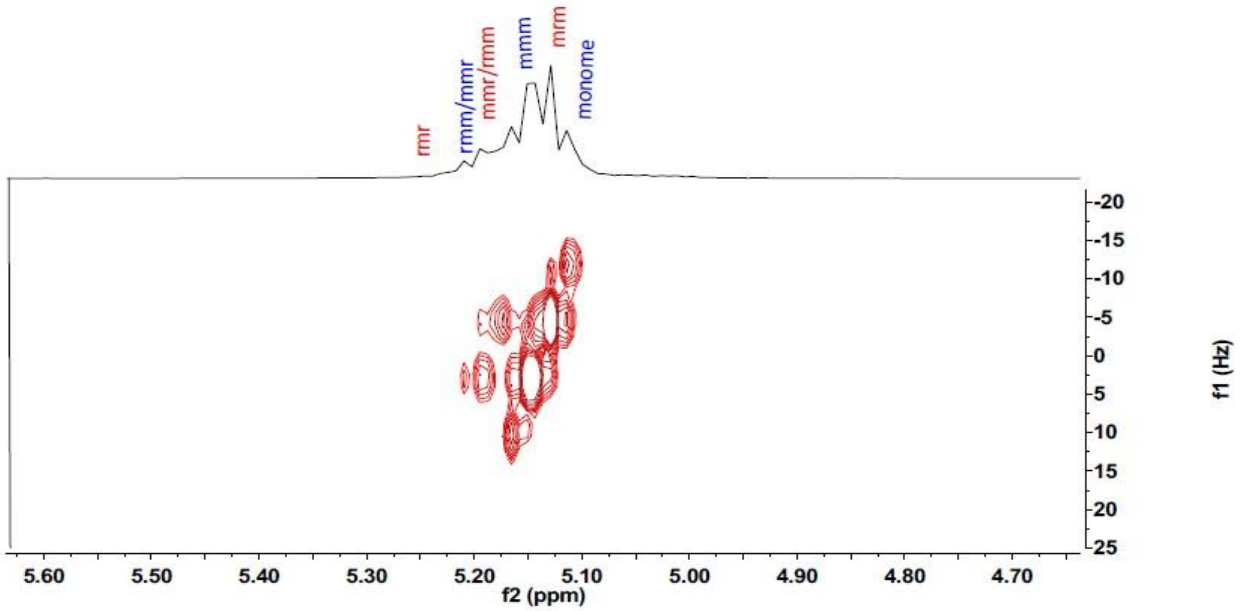

Figure S20. 2D J-resolved ^{1}H NMR spectrum of PLA (run 1, table 6).

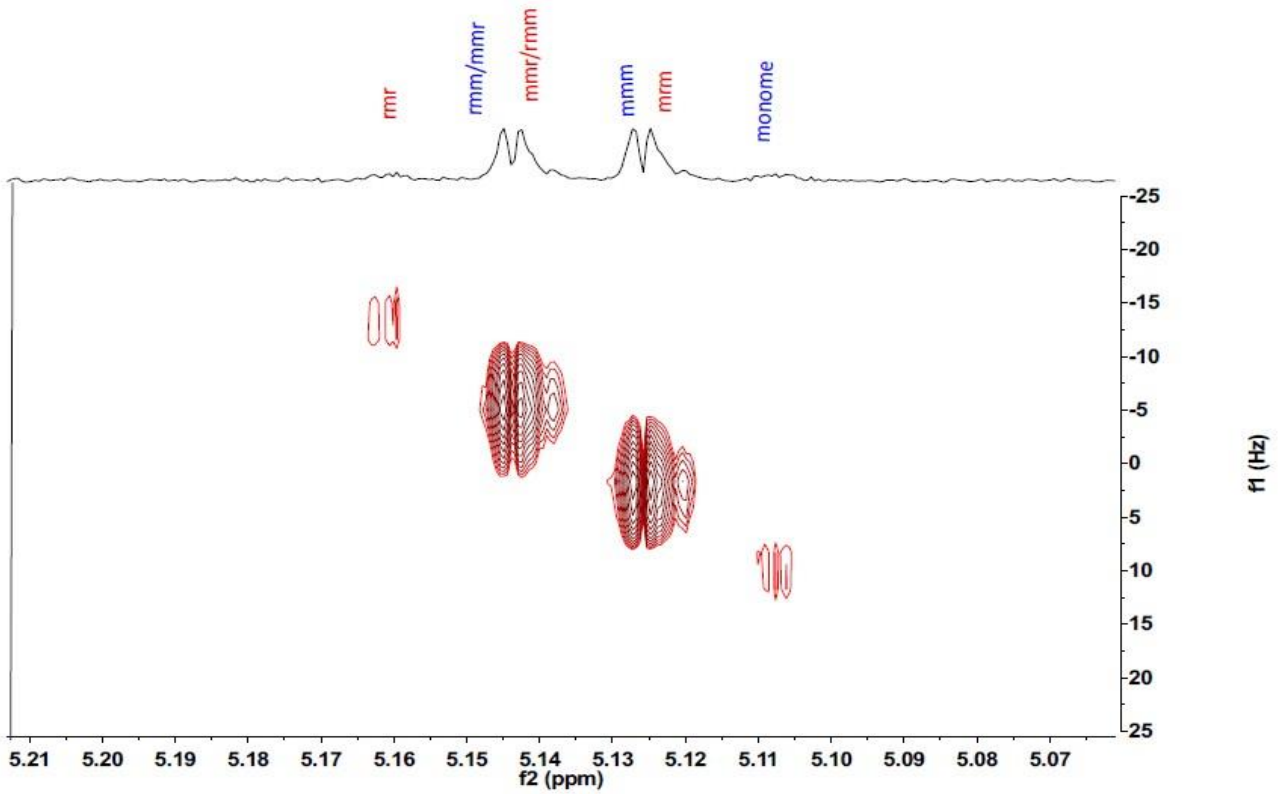

Figure S21. 2D J-resolved ^{1}H NMR spectrum of PLA (run x, table 6).

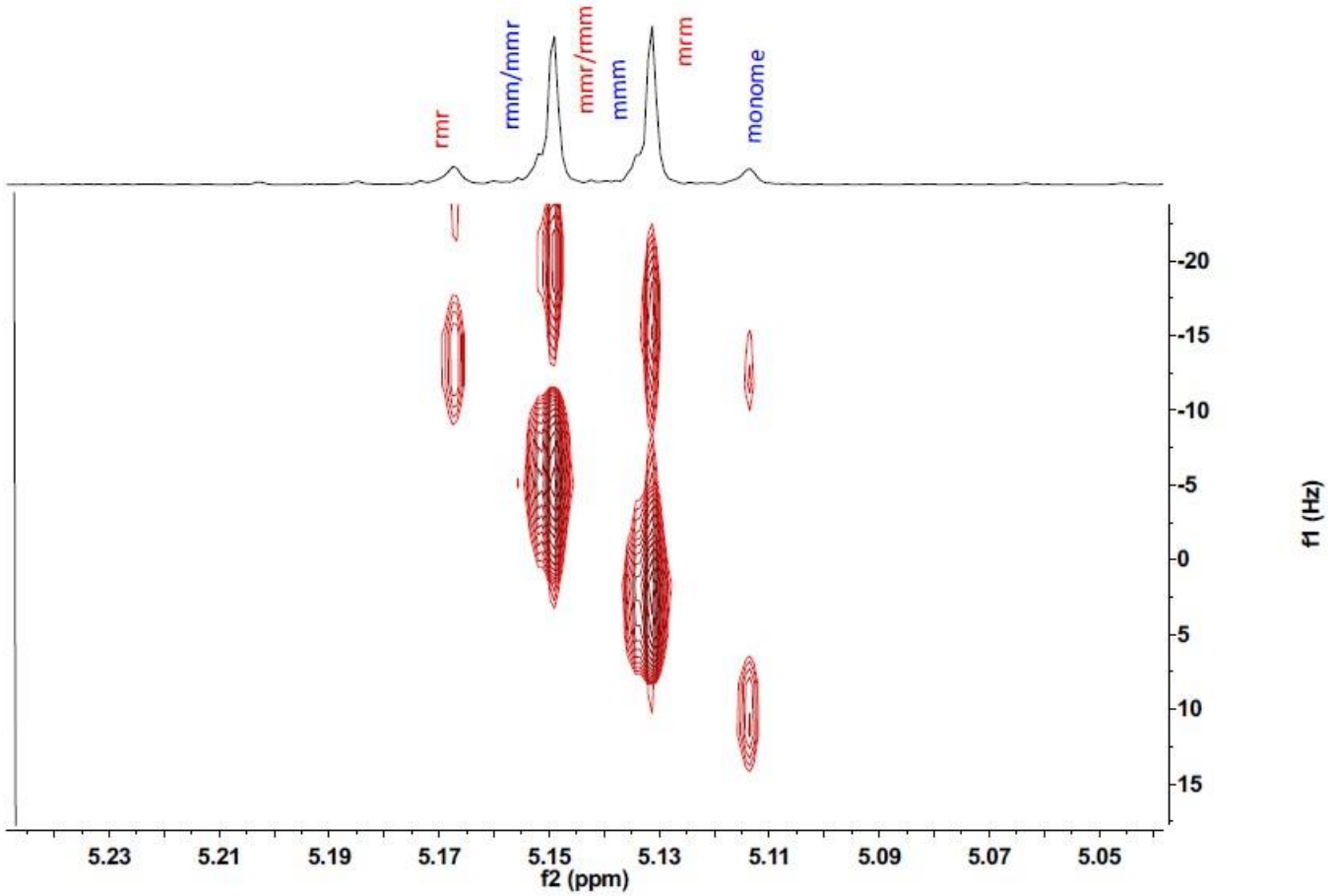

Figure S22. 2D J-resolved ^{1}H NMR spectrum of PLA (run 17, table 6).

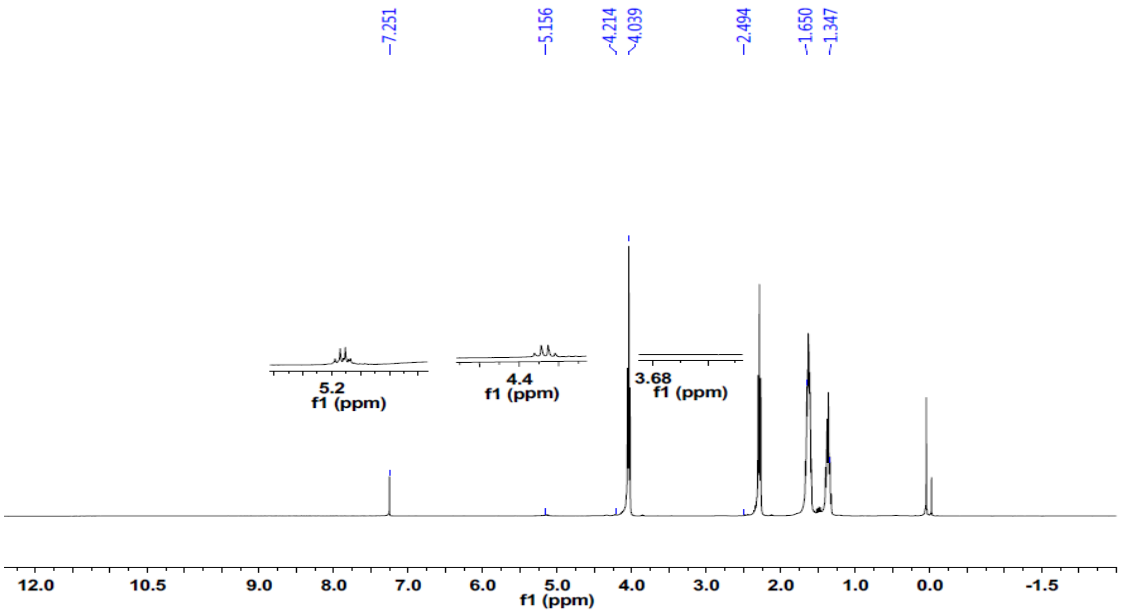

Figure S23. ^{1}H NMR spectrum of co-polymer from CL and *L*-LA (run 4, table 7).

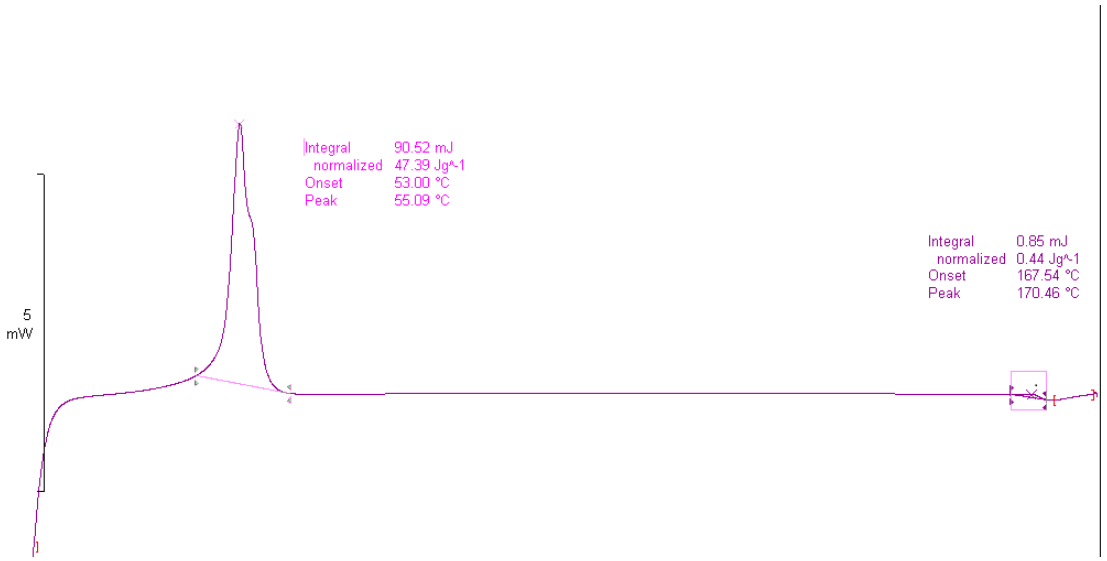

Figure S24. DSC plot of co-polymer from CL and *L*-LA (run 4, table 7).

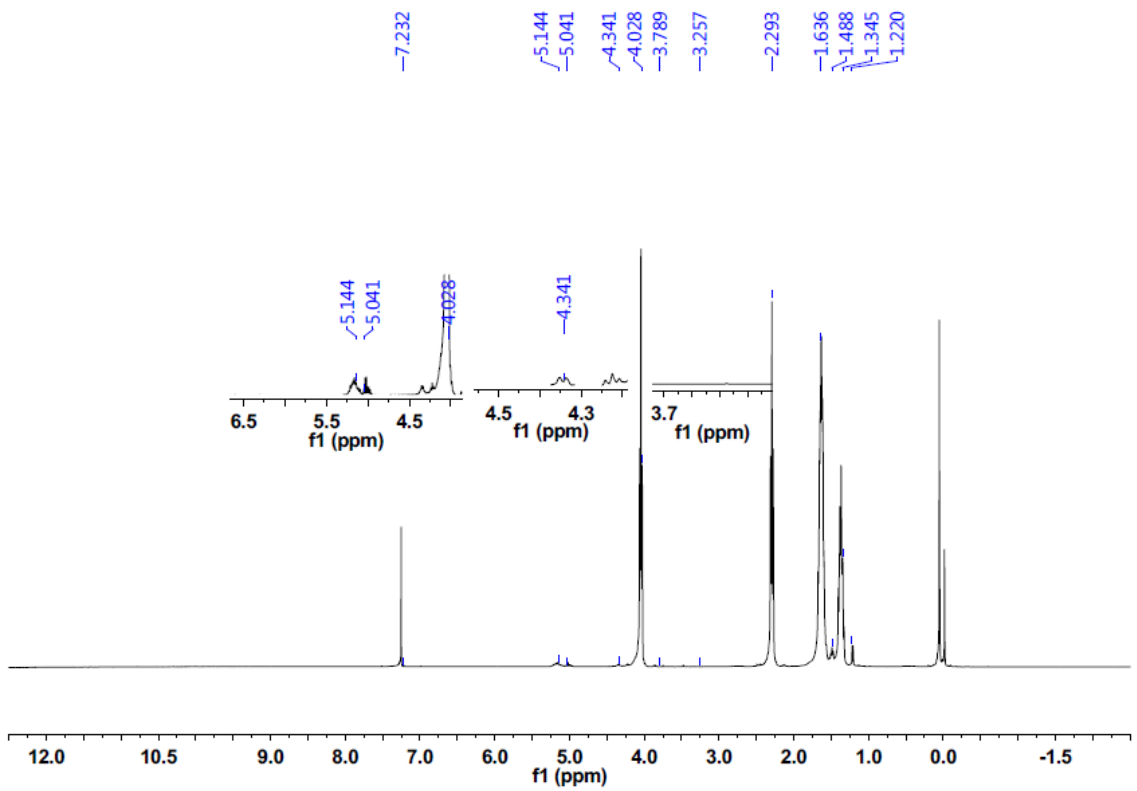

Figure S25. ^{1}H NMR spectrum of co-polymer from CL and *rac*-LA (run 6, table 8).

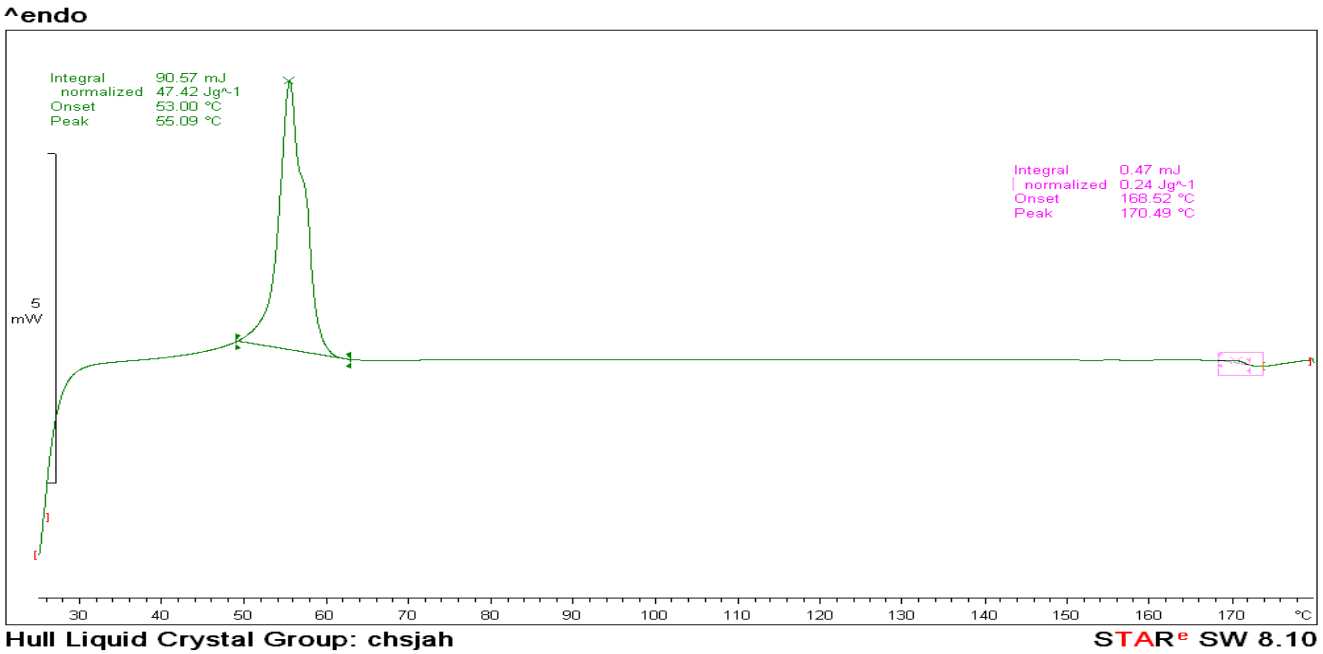

Figure S26. DSC plot of co-polymer from CL and *rac*-LA (run 4, table 8).

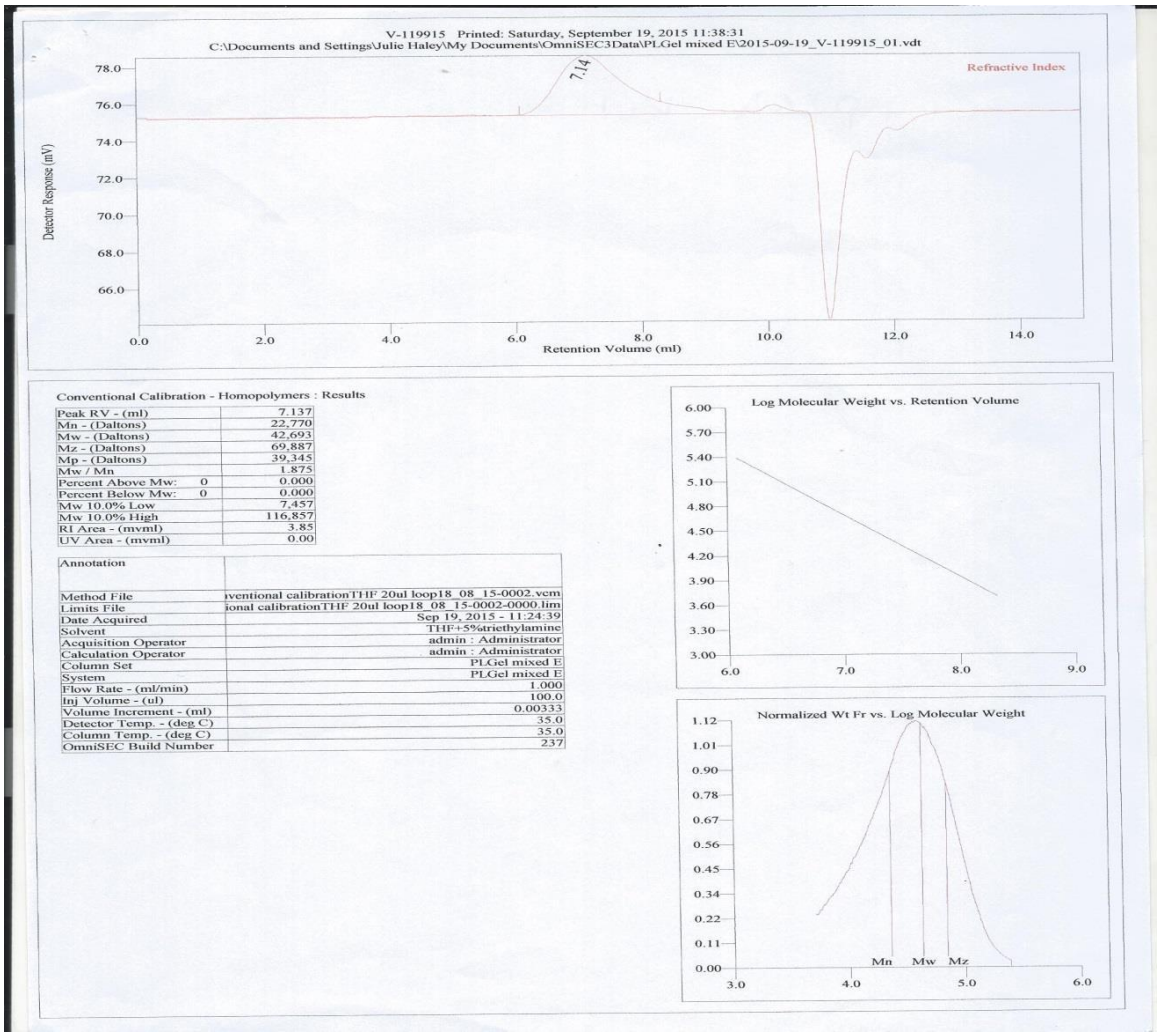

Figure S 27. GPC run 1 table 7

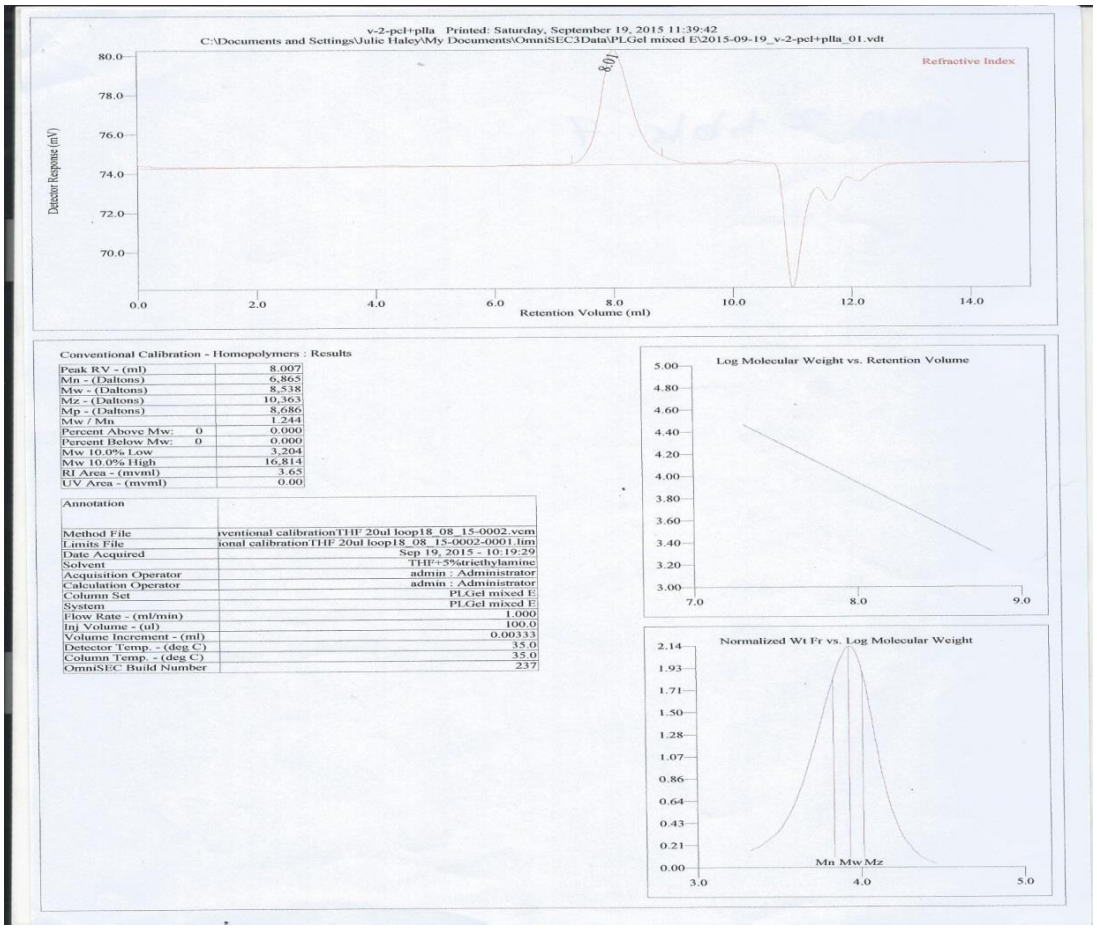

Figure S 28. GPC run 2 table 7

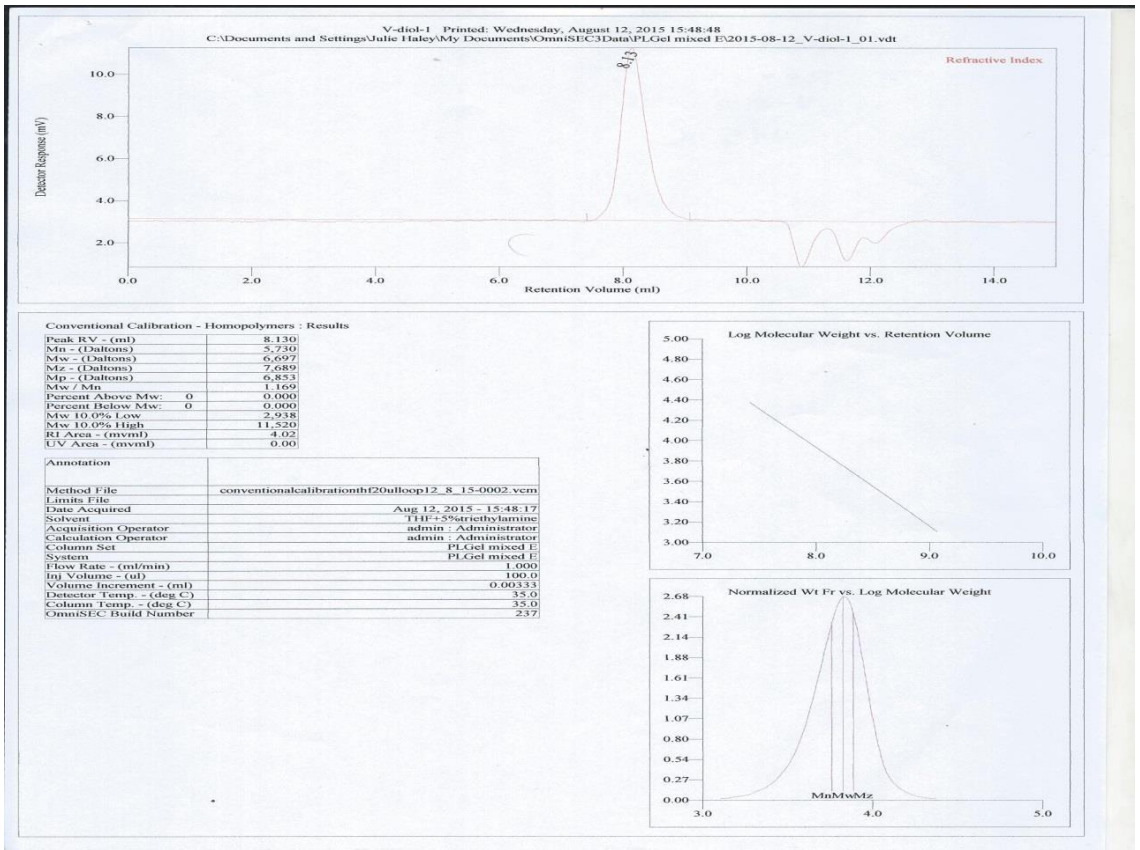

Figure S 29. GPC run 3 table 7

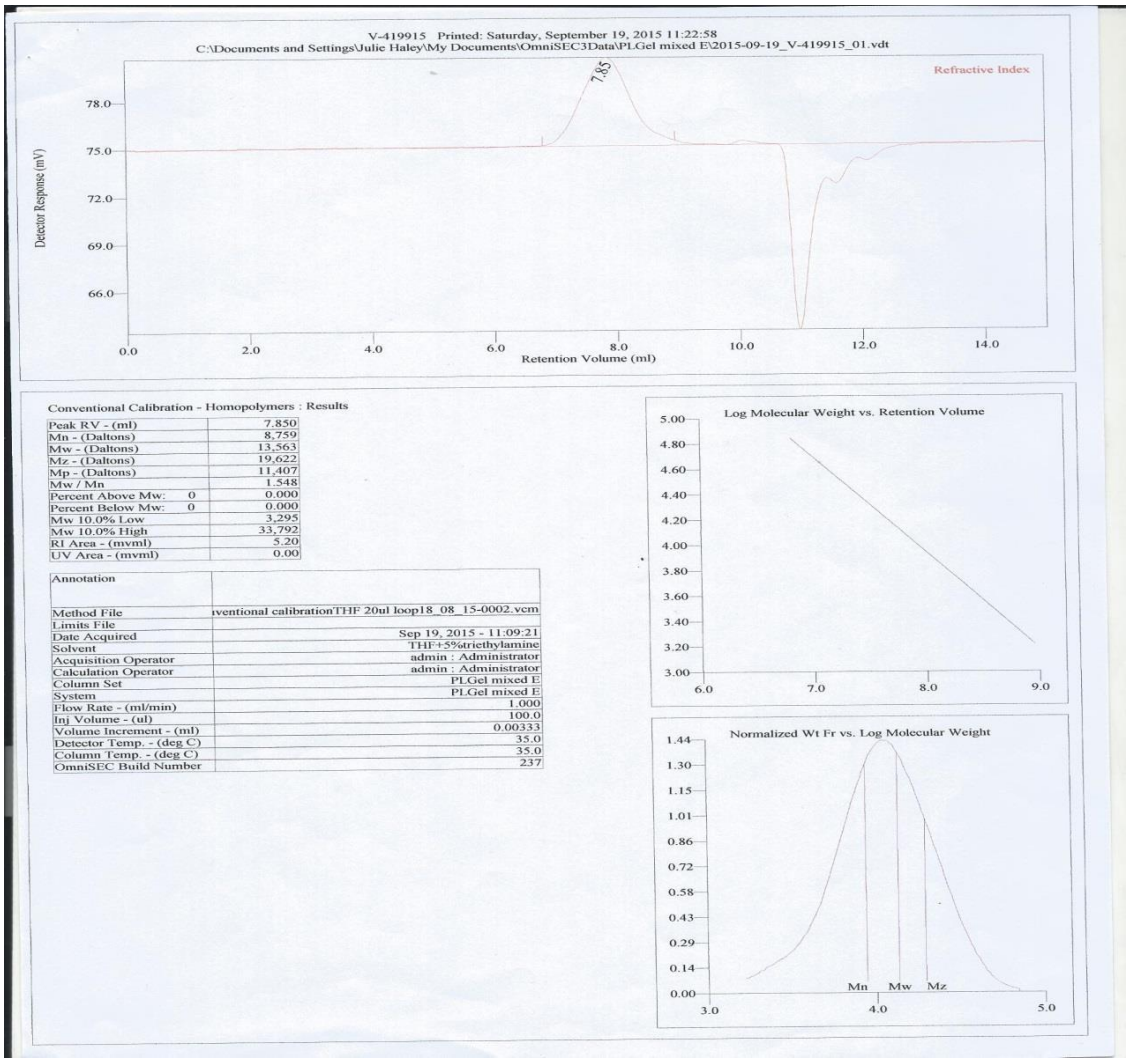

Figure S 30. GPC run 4 table 7

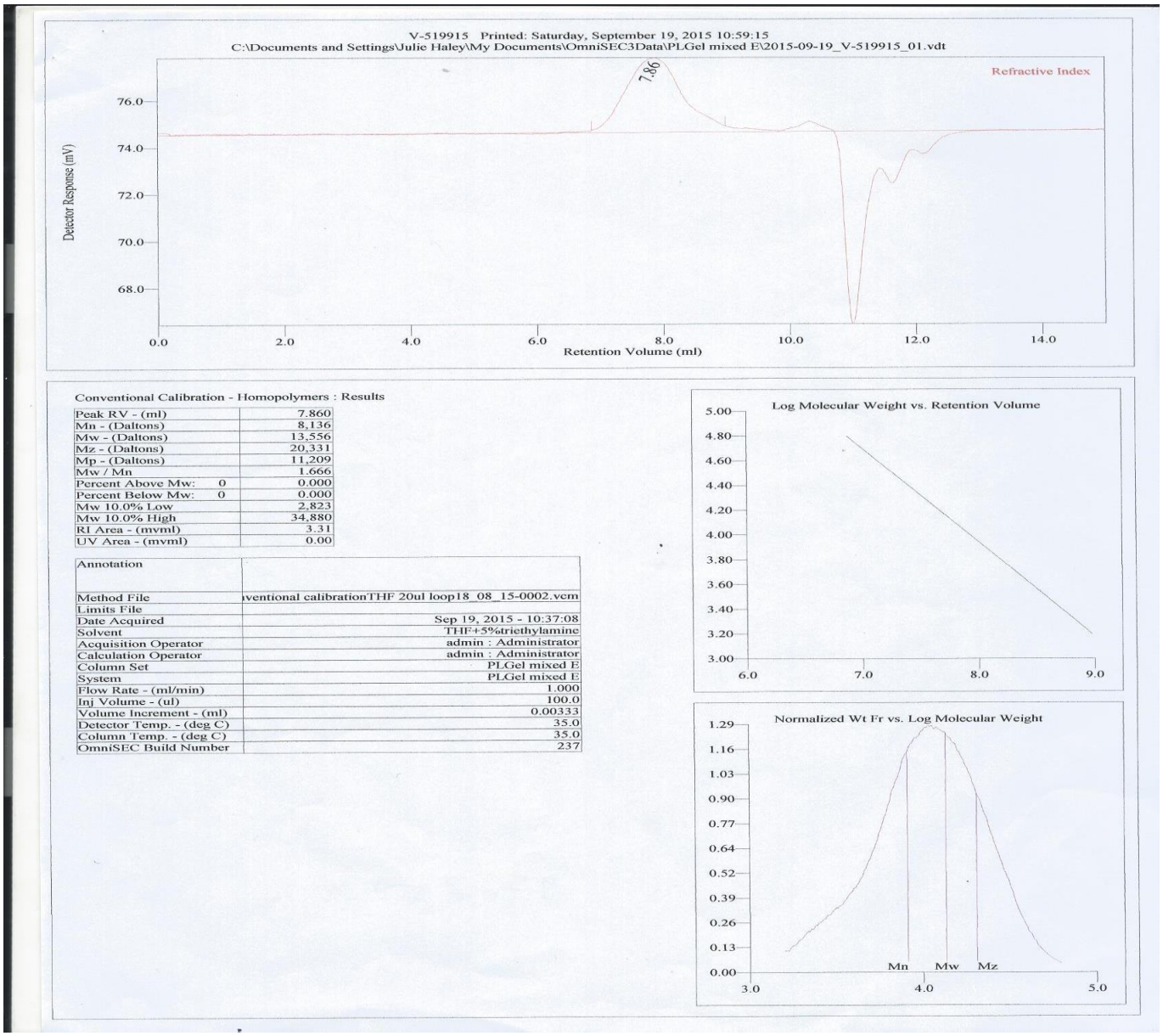

Figure S31. GPC run 5 table 7

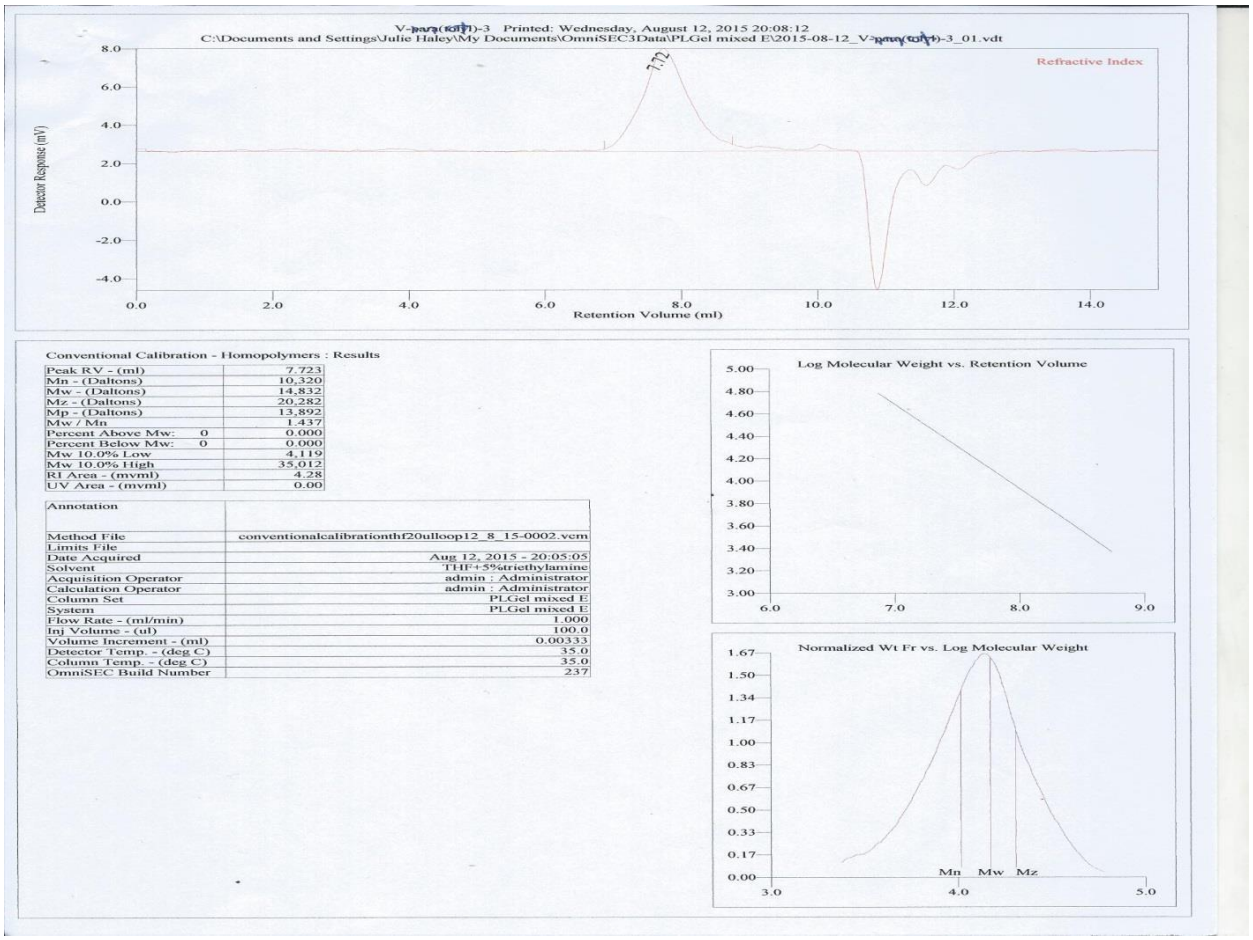

Figure S32. GPC run 6 table 7

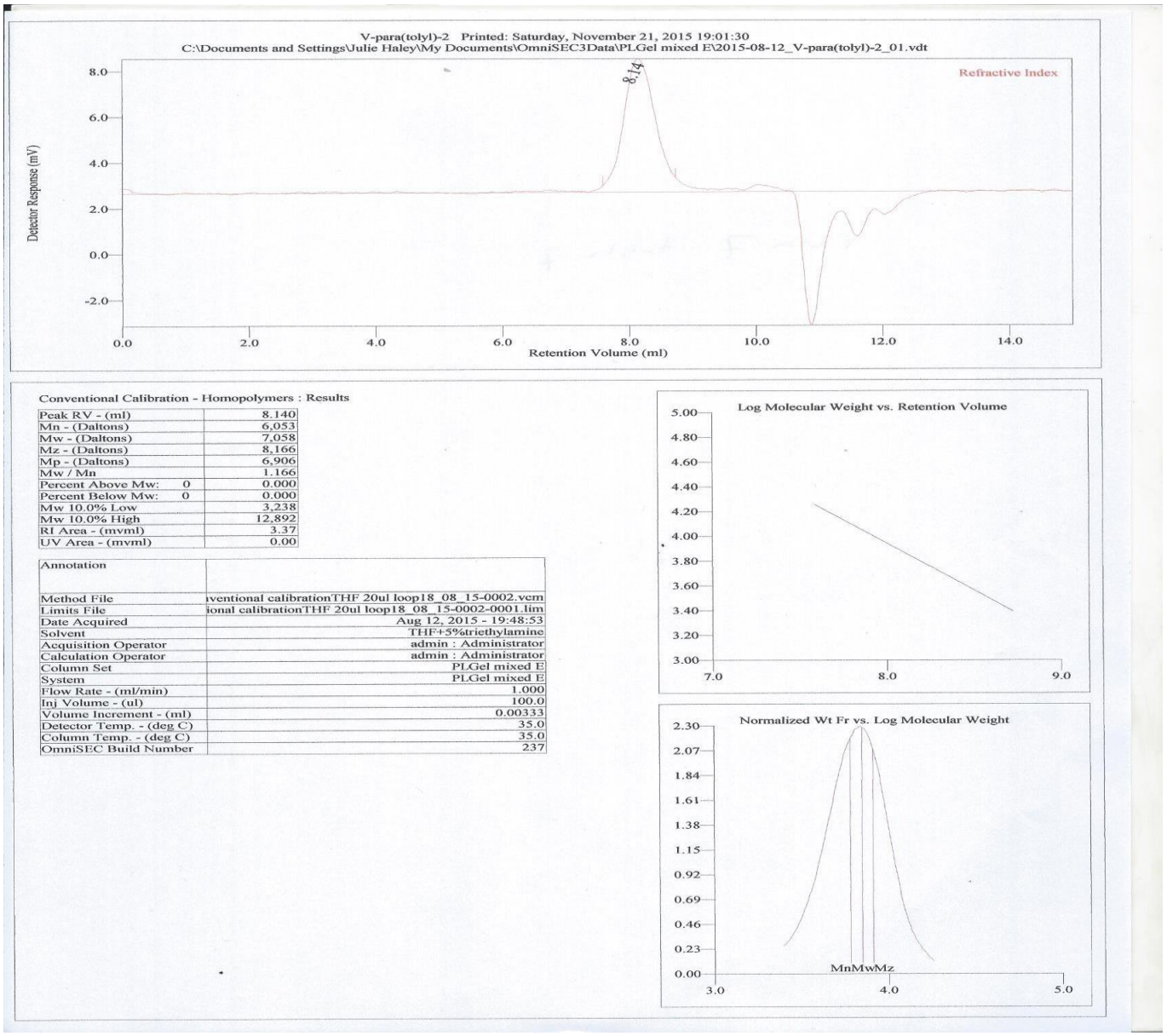

Figure S33. GPC run 7 table 7

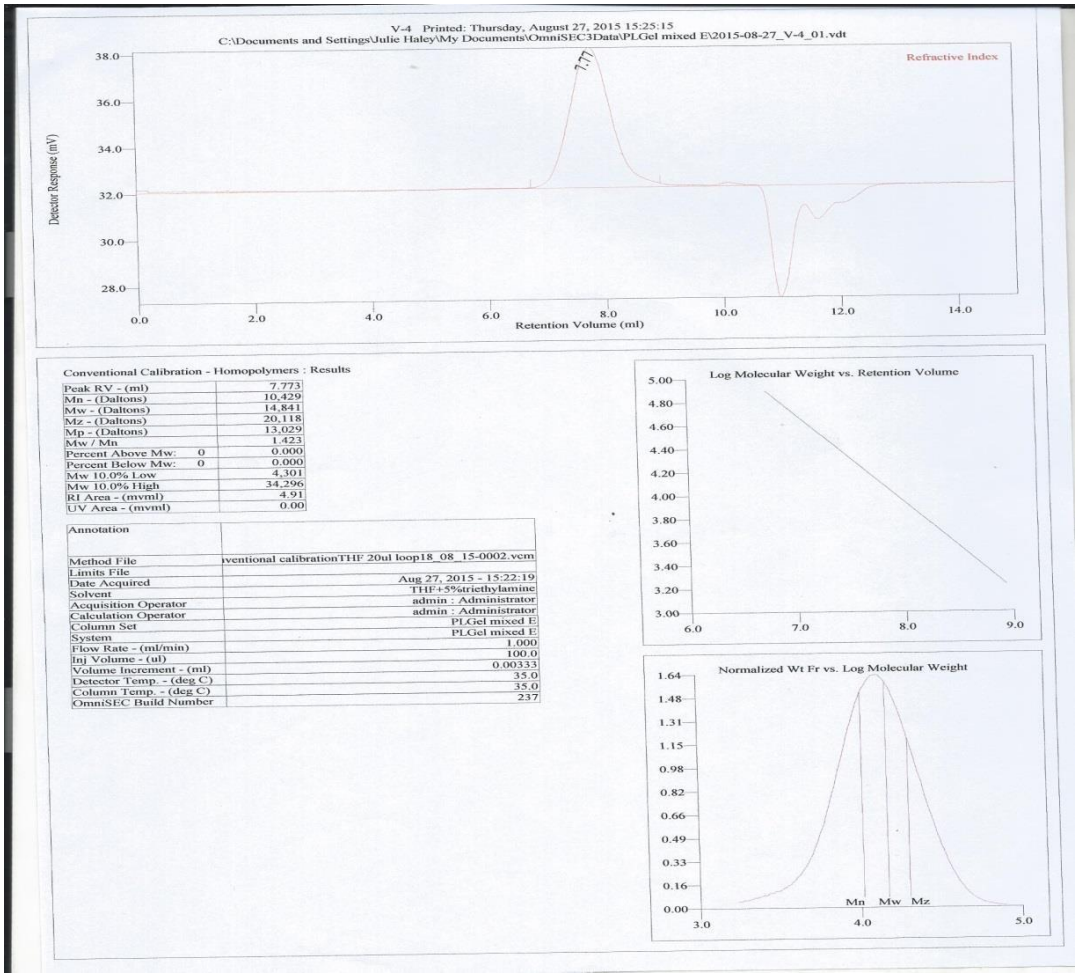

Figure S34. GPC run 1 table 8

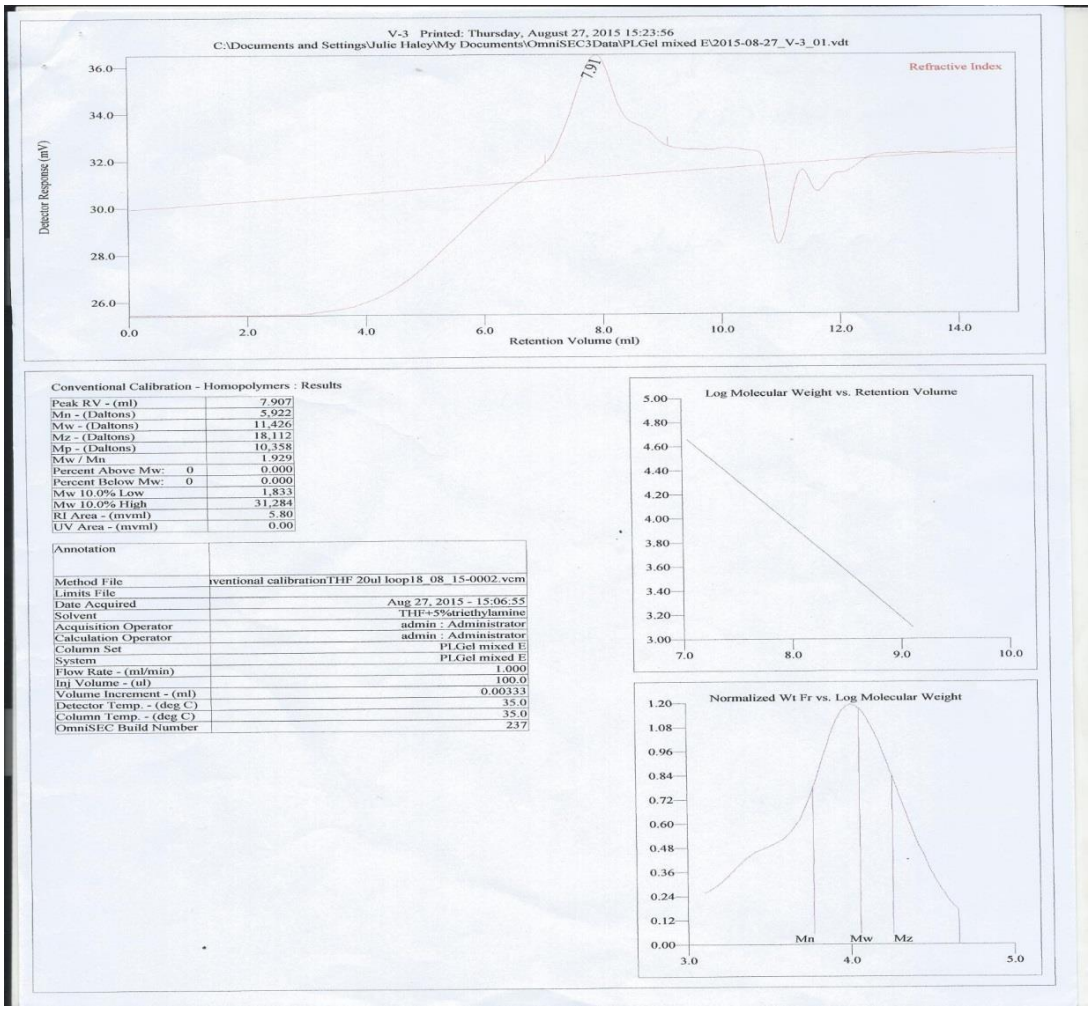

Figure S35. GPC run 2 table 8

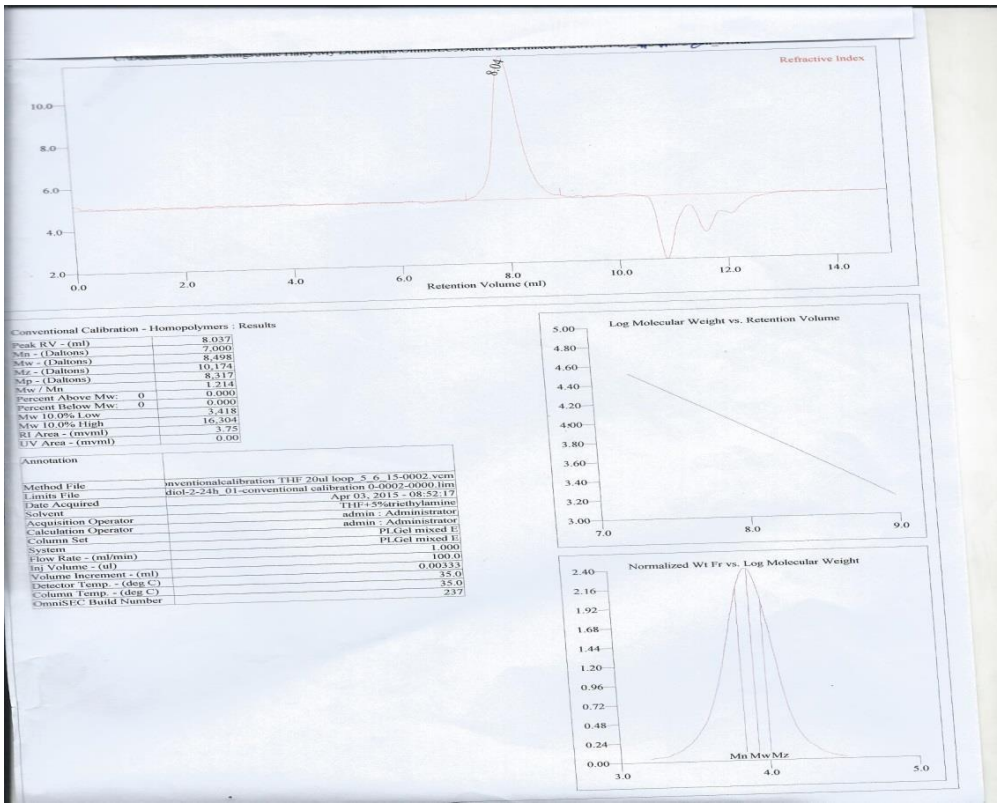

Figure S36. GPC run 3 table 8

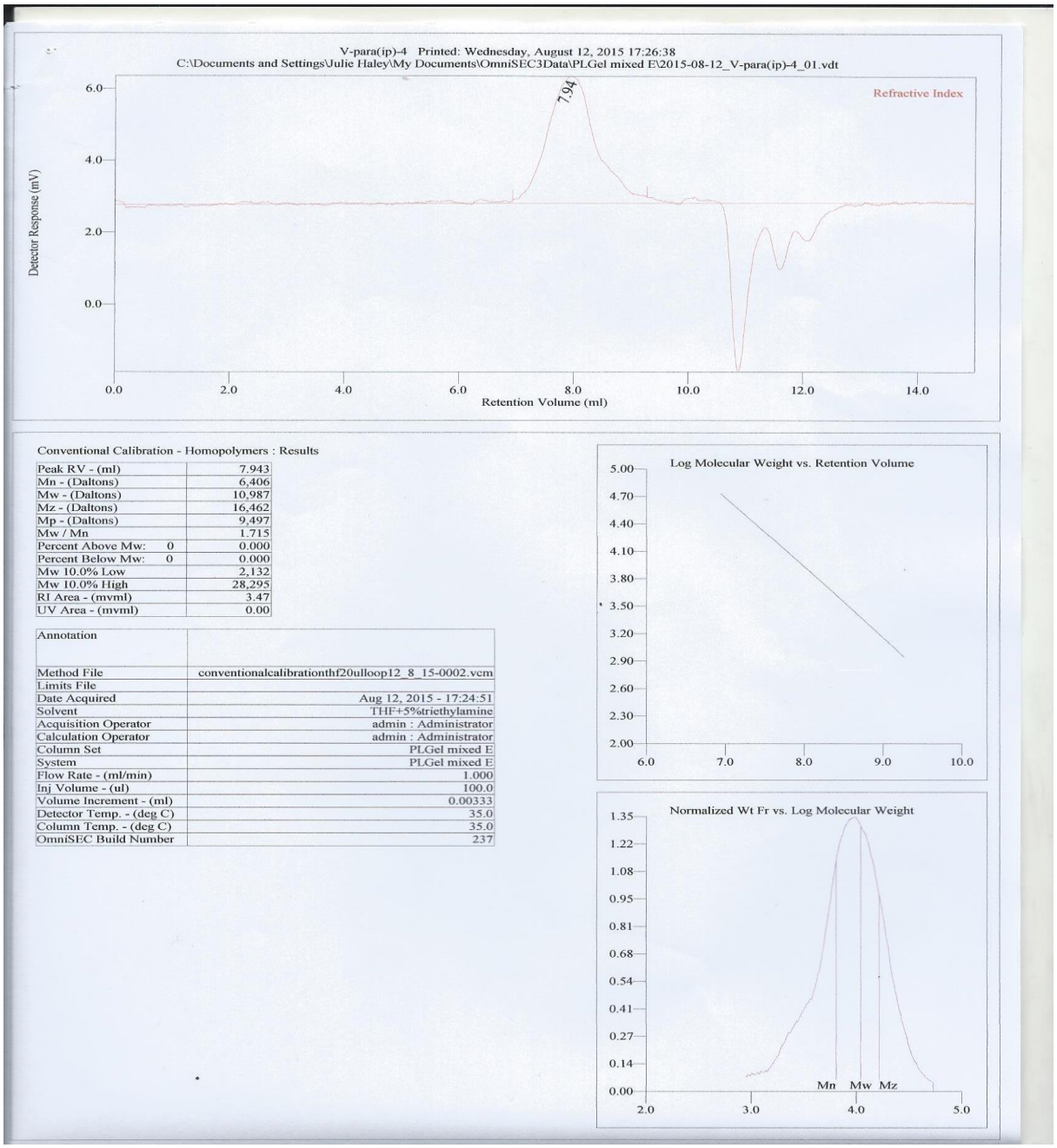

Figure S37. GPC run 4 table 8

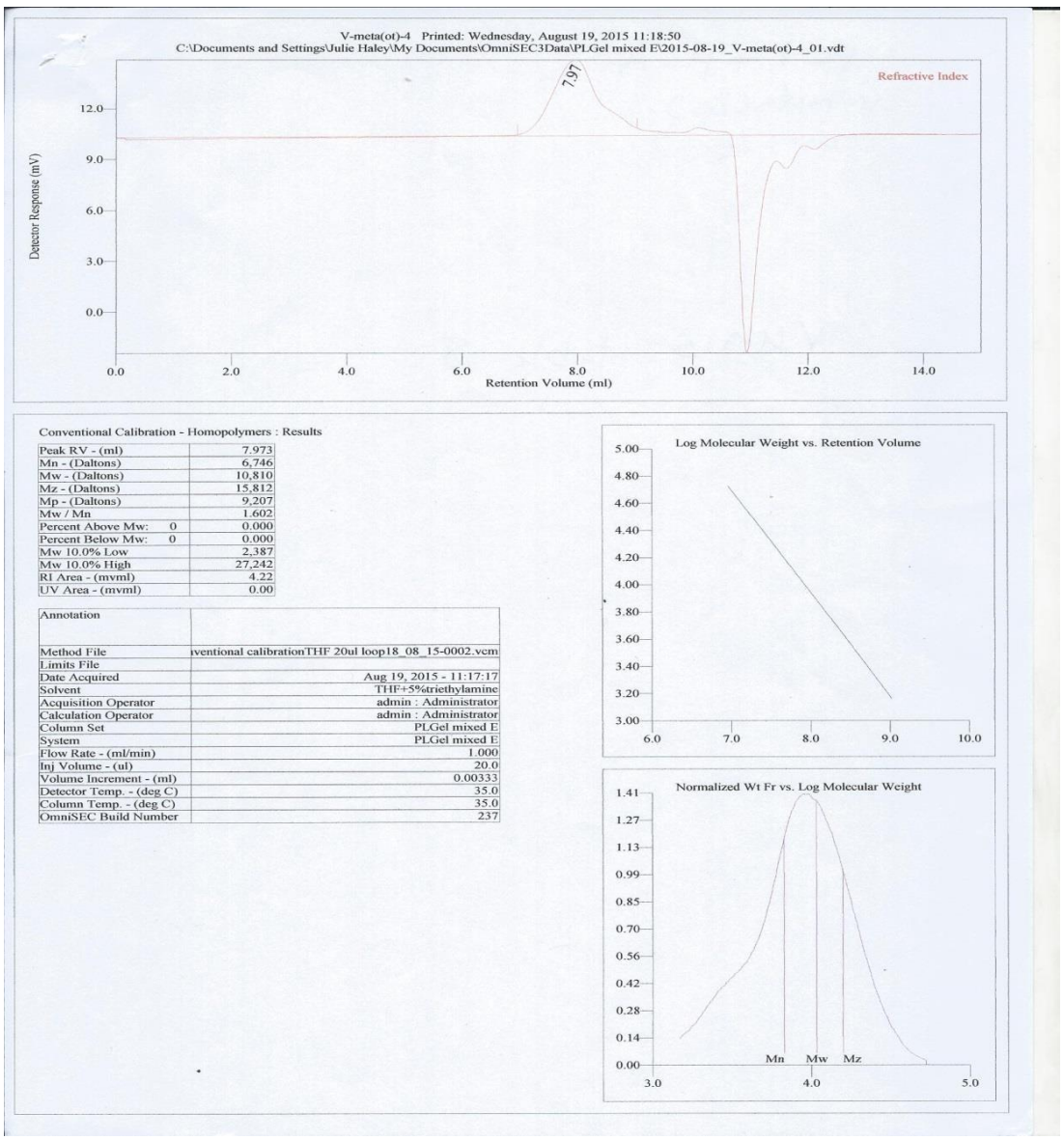

Figure S38. GPC run 5 table 8

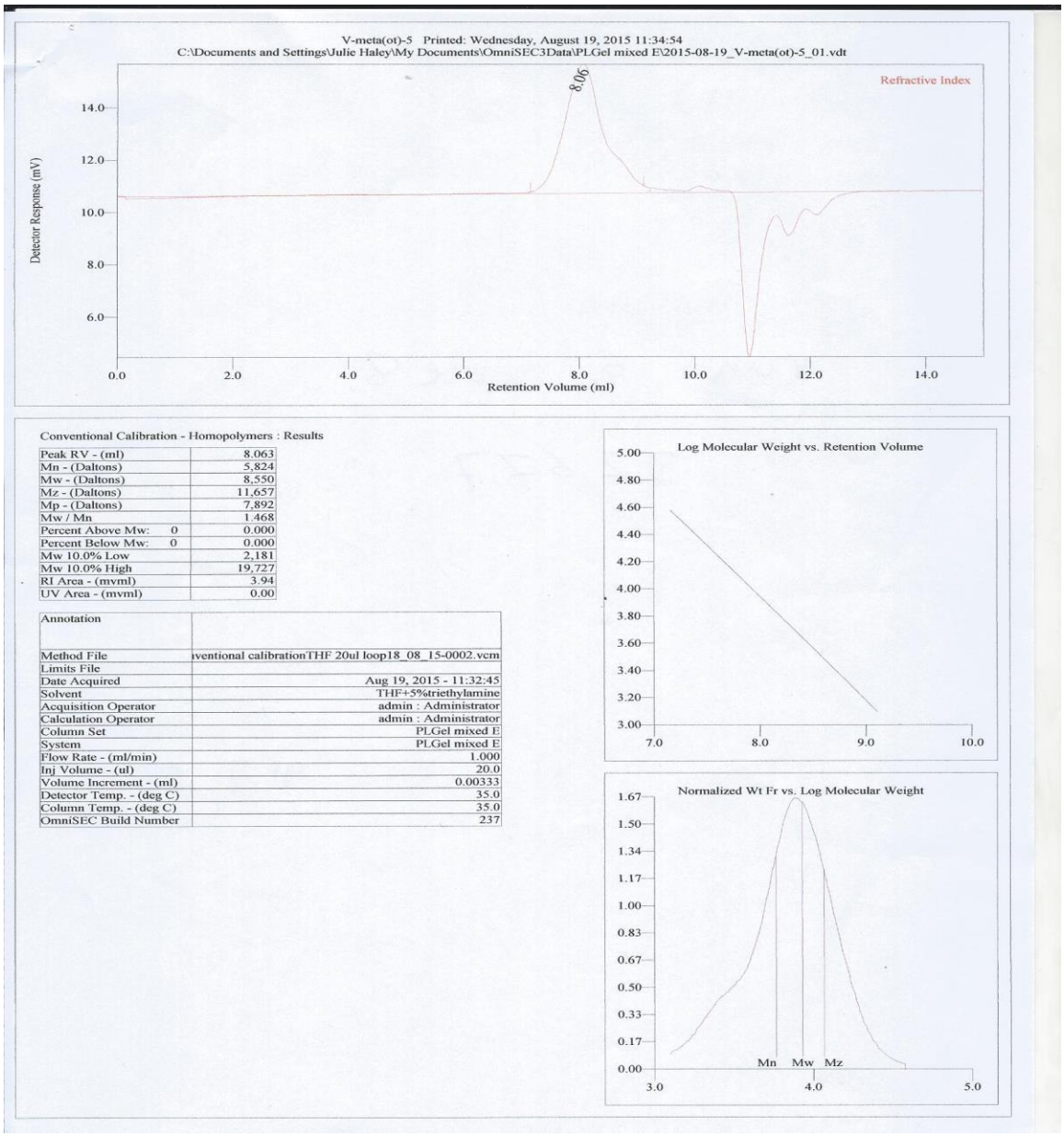

Figure S39. GPC run 6 table 8

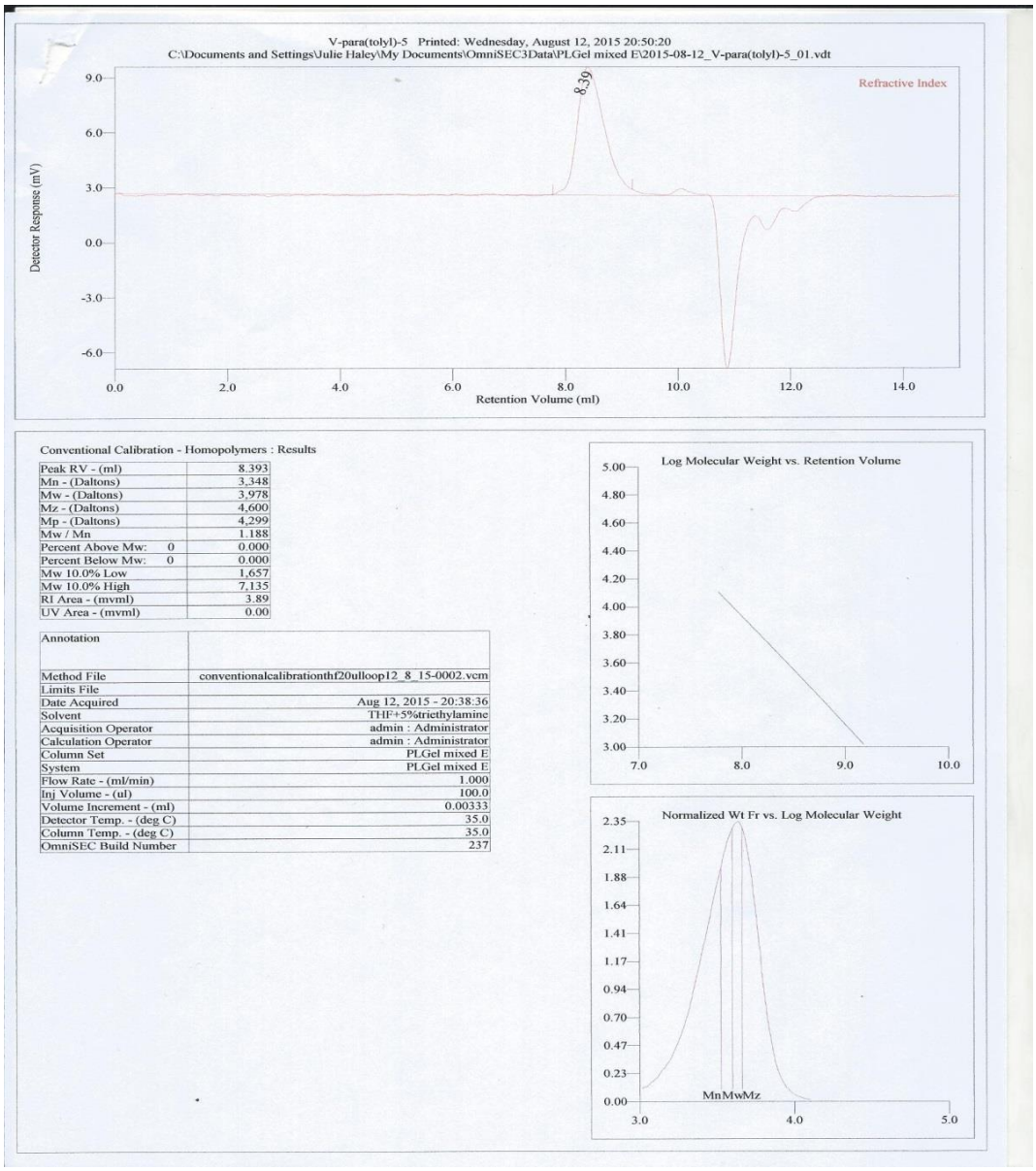

Figure S40. GPC run 7 table 8